



Adaptive Sampling, Data Assimilation and Adaptive Modeling



Pierre F.J. Lermusiaux

Division of Engineering and Applied Sciences, Harvard University



HU: A.R. Robinson, P.J. Haley, W.G. Leslie, O. Logoutov and X.S. Liang

Main collaborators
on this topic

AOSN2-MURI: N. Leonard, J. Marsden, S. Majumdar, Y. Chao

NSF-ITR: C. Evangelinos, R. Tian, N.K. Yilmaz, N. Patrikalakis

Uncertainty-DRI: C.-S. Chiu, P. Abbot, B. Miller

<http://www.deas.harvard.edu/~pierrel>

-
- 1. Oceanic Introduction and Error Subspace Statistical Estimation (ESSE)**
 - 2. Adaptive Sampling:** a) ESSE, b) MIP/ESSE, c) LCS, d) Collaborative control, e/f) Science
 - 3. Adaptive Modeling:** Forecast Error Analyses, Multi-model estimation and Adaptive physical-biogeochemical modeling
 - 4. Conclusions**

Processes/Platforms:

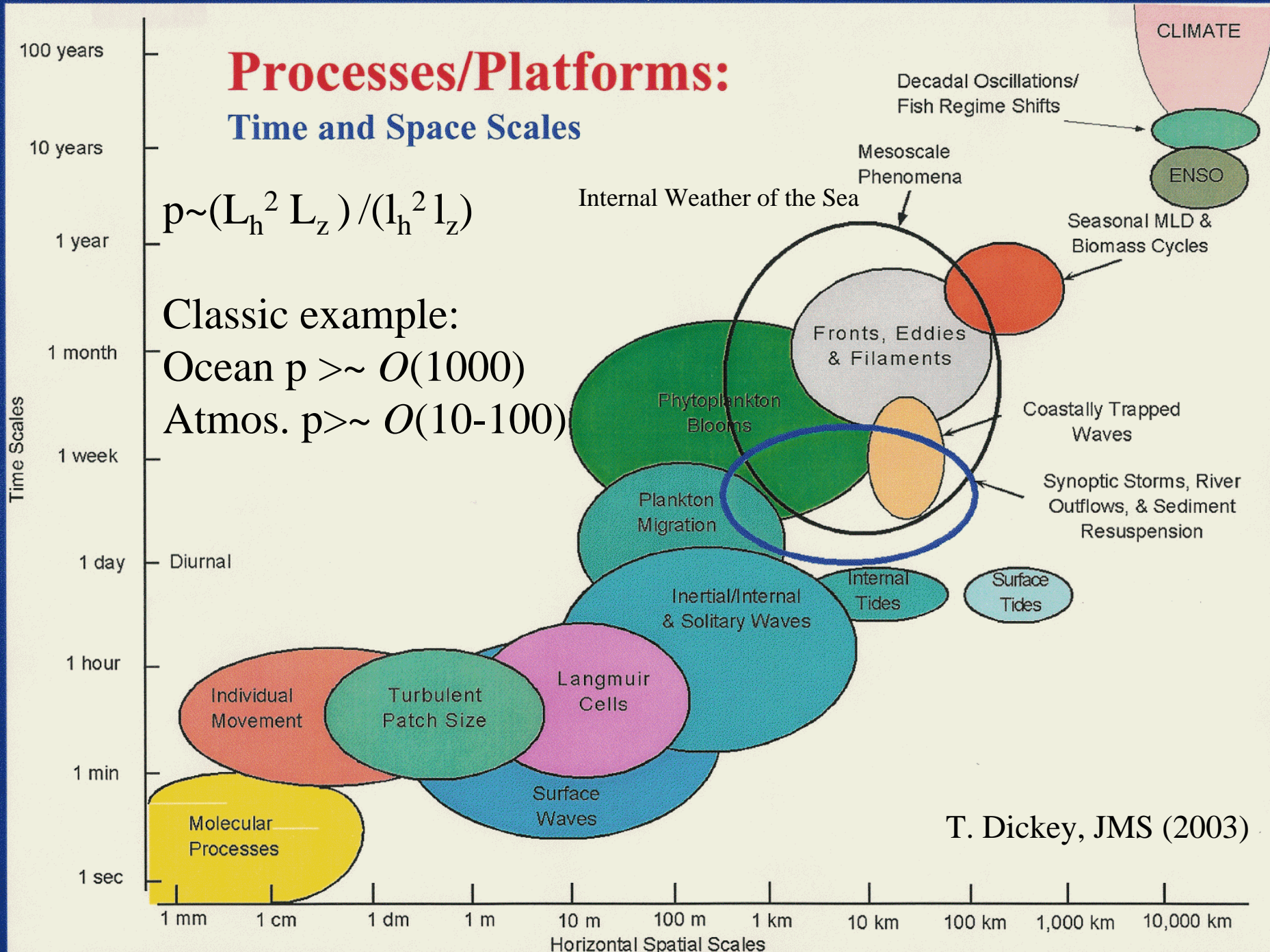
Time and Space Scales

$$p \sim (L_h^2 L_z) / (l_h^2 l_z)$$

Classic example:

Ocean $p > \sim O(1000)$

Atmos. $p > \sim O(10-100)$



T. Dickey, JMS (2003)

Physical and Multidisciplinary Observations

AUV



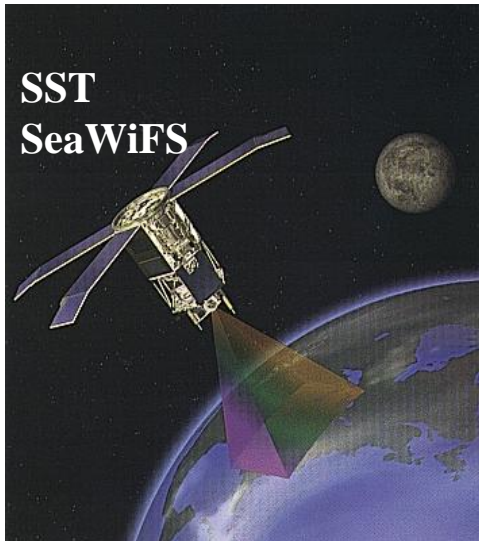
Aircraft



Ships



Satellite



Moored/Fixed

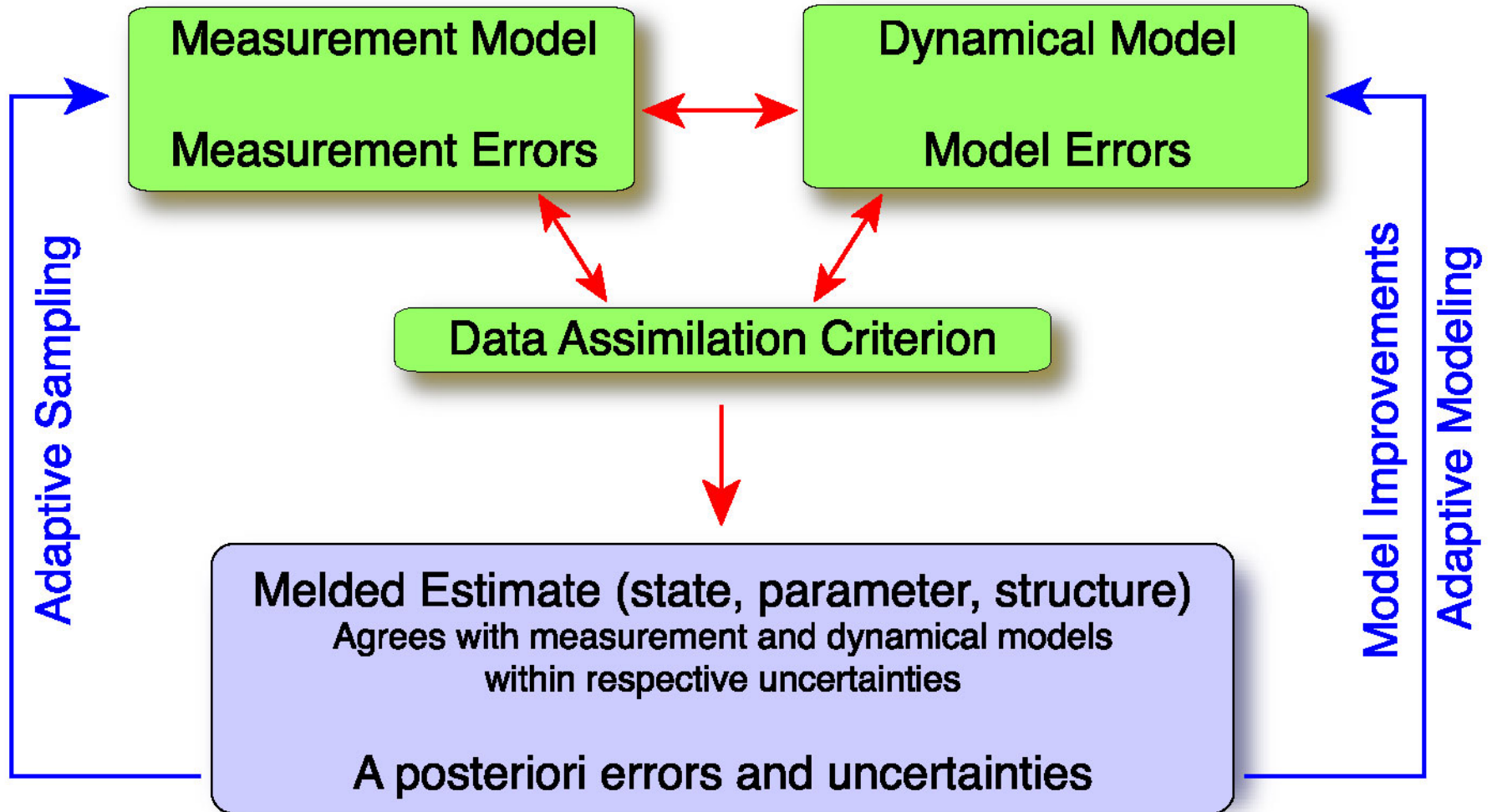


Drifting



WHAT IS DATA ASSIMILATION?

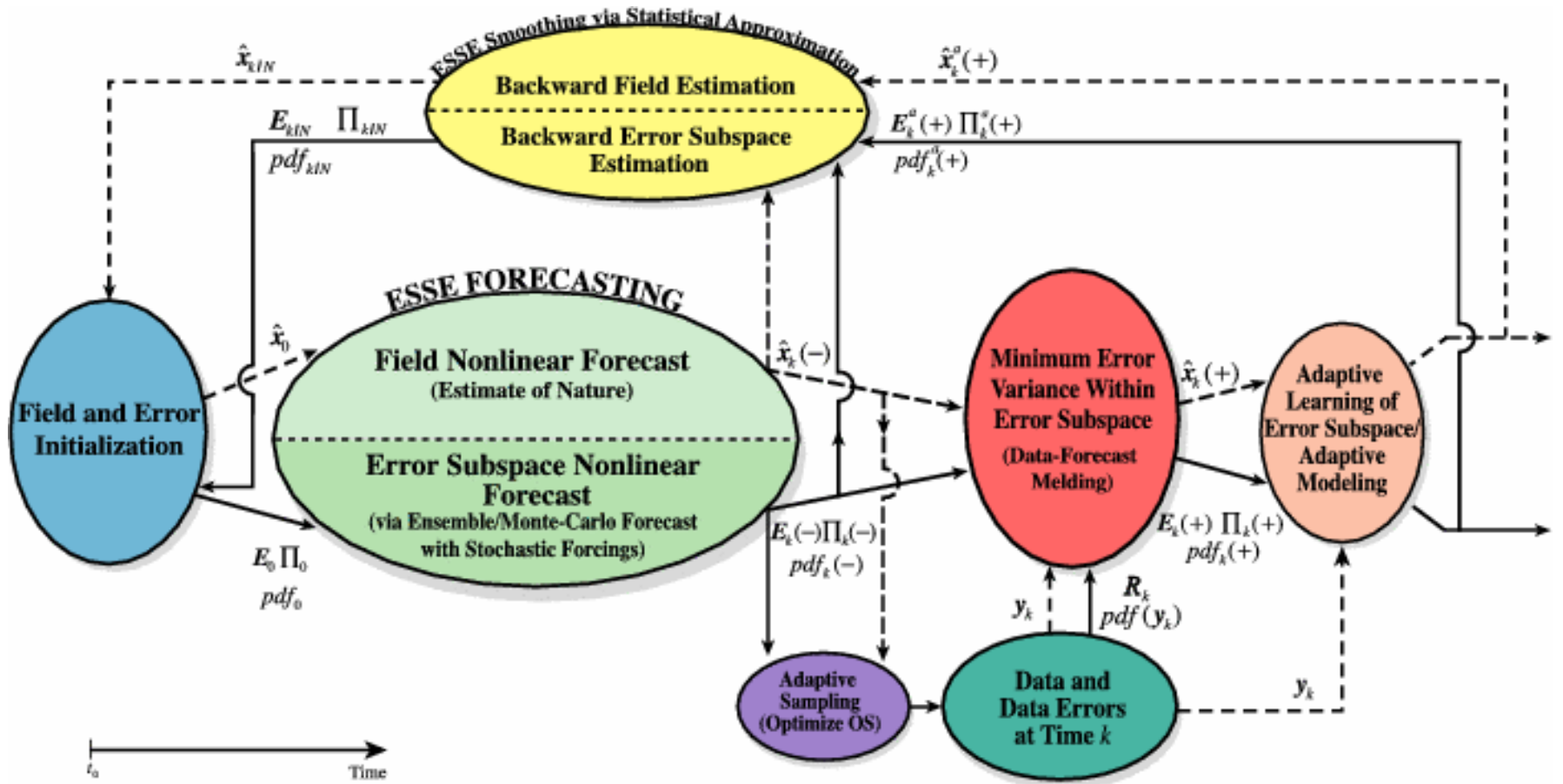
A Melded Estimate of Data and Dynamics



e.g. Robinson A.R., P.F.J. Lermusiaux and N.Q. Sloan, III (1998). *Data Assimilation*. The Sea, Vol. 10.

Robinson A.R. and P.F.J. Lermusiaux (2002). *DA for physical-biological interactions*. The Sea, Vol.12

Error Subspace Statistical Estimation (ESSE)



- Uncertainty forecasts (with dynamic error subspace, error learning)
- Ensemble-based (with nonlinear and stochastic primitive eq. model (HOPS))
- Multivariate, non-homogeneous and non-isotropic Data Assimilation (DA)
- Consistent DA and adaptive sampling schemes
- Software: not tied to any model, but specifics currently tailored to HOPS

Ocean Regions and Experiments/Operations for which ESSE has been utilized in real-time

- Strait of Sicily (AIS96-RR96), Summer 1996
- Ionian Sea (RR97), Fall 1997
- Gulf of Cadiz (RR98), Spring 1998
- Massachusetts Bay (LOOPS), Fall 1998
- Georges Bank (AFMIS), Spring 2000
- Massachusetts Bay (ASCOT-01), Spring 2001
- Monterey Bay (AOSN-2), Summer 2003

For publications, email me or see <http://www.deas.harvard.edu/~pierrel>

Data Assimilation via ESSE

Table 1. Filtering/Smoothing via ESSE: Continuous-Discrete Problem Statement

Dynamical Model:	$d\hat{\mathbf{x}} = \mathcal{M}(\hat{\mathbf{x}}) dt + d\hat{\boldsymbol{\eta}}, \text{ with } \hat{\mathbf{x}}(\mathbf{r}_0, t_0) = \hat{\mathbf{x}}_0 + \hat{\mathbf{n}}(0).$
Measurement Model:	$\mathbf{y}_k^o = \mathcal{H}(\mathbf{x}_k) + \hat{\boldsymbol{\epsilon}}_k.$
Estimation Criterion:	
Estimate	
Error Subspace:	$\left\{ \text{Find } \mathbf{P}_k^p = \mathbf{E}_k \boldsymbol{\Pi}_k \mathbf{E}_k^T \text{ with } \text{rank}(\mathbf{E}_k) = p \mid \min_{\boldsymbol{\Pi}_k, \mathbf{E}_k} \ \mathbf{P}_k - \mathbf{P}_k^p\ \right\}$
Estimate State by	
Min. Err. Var. in ES:	$\left\{ \text{Find } \hat{\mathbf{x}}_k \mid \min_{\hat{\mathbf{x}}_k} J_k = \text{tr} [\mathbf{P}_k^p(+)] \text{ using } [\mathbf{y}_0^o, \dots, \mathbf{y}_k^o / \mathbf{y}_N^o] \right\}$

○ **Optimal error space reduction and Min. Err. Var. combined:**

“Estimate the ocean evolution by minimizing the largest (most energetic) expected errors, in agreement with the full dynamical model and measurement model (data) constraints, and their respective uncertainties.”

○ Linked to POD/Polynomial Chaos, but with

time-varying error Karhunen-Loeve basis:
$$\mathbf{x}(x, t, \theta) = \bar{\mathbf{x}}(x, t) + \sum_{i=1}^M \sqrt{\lambda_i} \phi_u^s(\mathbf{x}, t) \zeta_i(\theta)$$

Nonlinear Dynamical State and Error Subspace Ensemble Forecast

for Sequential Statistical Estimation

- **Cond. Mean Estimates:**

Central forecast: $\hat{\mathbf{x}}_{k+1}^{cf}(-) \mid d\hat{\mathbf{x}} = \mathcal{M}(\hat{\mathbf{x}}, t) dt$, with $\hat{\mathbf{x}}_k = \hat{\mathbf{x}}_{k(+)}$.

Ensemble mean: $\hat{\mathbf{x}}_{k+1}^{em}(-) \doteq \mathcal{E}^q \{ \hat{\mathbf{x}}_{k+1}^j(-) \}$.

- **ES Initial Conditions:**

$\hat{\mathbf{x}}_k^j(+) = \hat{\mathbf{x}}_k(+) + \mathbf{E}_{k(+)} \boldsymbol{\pi}_k^j(+) + n_k^j$, $j = 1, \dots, q$,

with either,

$$\boldsymbol{\pi}_k^j(+) = \mathbf{\Pi}_k^{\frac{1}{2}}(+) \mathbf{u}^j,$$

$$\boldsymbol{\pi}_k^j(+) = \mathbf{\Pi}_k^{\frac{1}{2}}(+) \mathbf{u}^j, \text{ with dynamical/dataconstraints, or,}$$

$$\boldsymbol{\pi}_k^j(+) = \boldsymbol{\Sigma}(+) (\mathbf{V}_+^T)^j, \text{ with (32) or (33a-c),}$$

where \mathbf{u} is of zero mean and covariance \mathbf{I}^p .

- **Ensemble Forecast:**

$\hat{\mathbf{x}}_{k+1}^j(-) \mid d\hat{\mathbf{x}}^j = \mathcal{M}(\hat{\mathbf{x}}^j, t) dt + d\mathbf{w}$, with $\hat{\mathbf{x}}_k^j = \hat{\mathbf{x}}_k^j(+)$, $j = 1, \dots, q$.

where $\mathcal{E} \{ d\mathbf{w}(t) d\mathbf{w}^T(t) \} \doteq \mathbf{Q}(t) dt \doteq \mathbf{B}(t) \mathbf{B}^T(t) dt$ and $\mathbf{B}(t) \in \mathbb{R}^{n \times r}$.

- **ES Forecast:**

$\mathbf{M}_{k+1}(-) = [\hat{\mathbf{x}}_{k+1}^j(-) - \hat{\mathbf{x}}_{k+1}(-)]$, $j = 1, \dots, q$,

decomposed into, $\mathbf{\Pi}_{k+1}(-) \doteq \frac{1}{q} \boldsymbol{\Sigma}_{k+1}^2(-)$ and $\mathbf{E}_{k+1}(-)$ of rank $p \leq q$, where,

$$\left\{ \boldsymbol{\Sigma}_{k+1}(-), \mathbf{E}_{k+1}(-) \mid \text{SVD}_p(\mathbf{M}_{k+1}(-)) = \mathbf{E}_{k+1}(-) \boldsymbol{\Sigma}_{k+1}(-) \mathbf{V}_{k+1}^T(-) \right\}$$

and the operator $\text{SVD}_p(\cdot)$ selects the rank- p SVD.

- **Convergence Crit.:**

$$\rho = \frac{\sum_{i=1}^k \sigma_i(\mathbf{\Pi}^{\frac{1}{2}} \mathbf{E}^T \tilde{\mathbf{E}} \tilde{\mathbf{\Pi}}^{\frac{1}{2}})}{\sum_{i=1}^{\tilde{p}} \sigma_i(\tilde{\mathbf{\Pi}})} \geq \alpha,$$

where α is a chosen convergence limit ($1 - \epsilon \leq \alpha \leq 1$),

$k = \min(\tilde{p}, p)$ and

$\sigma_i(\cdot)$ selects the singular value number i .

STOCHASTIC FORCING MODEL: Sub-grid-scales

I. 0d Random Noise Exponentially Decorrelated in Time

$$d\tilde{w} + \beta \tilde{w} dt = dw, \quad (76)$$

$$\dot{p}_{\tilde{w}} = -2\beta p_{\tilde{w}} + q . \quad (77)$$

Setting $\dot{p}_{\tilde{w}}$ to zero at all times yields $p_{\tilde{w}}(0) = \sigma^2 = \frac{q}{2\beta}$. The process \tilde{w} is assumed to be of fixed fluctuation amplitude σ and autocorrelation time $\frac{1}{\beta}$. The constant variance of the white noise w is thus set to $q = 2\beta\sigma^2$.

II. 3d Random Noise, Exponentially Decorrelated in Time and 2-Grid Point Decorrelated in Space

$$d\psi^t = \mathbf{f}^{PE}(\psi^t, t) dt + \mathbf{B}^{fc}(t) d\tilde{\mathbf{w}}^c . \quad (86a)$$

$$d\tilde{\mathbf{w}}^c = -\beta^c \tilde{\mathbf{w}}^c dt + d\mathbf{w}^c , \quad (86b)$$

where symbols denote the:

- discrete-space PE state vector: $\psi = (\hat{\mathbf{u}}, \hat{\mathbf{v}}, \mathbf{T}, \mathbf{S}, \mathbf{p})^T \in \mathbb{R}^n$
- coarse 3d white noise: \mathbf{w}_k^c
- Coarse 3d Gauss-Markov process: $\tilde{\mathbf{w}}_k^c$,
 i.e. $d\mathbf{w}^c = (d\mathbf{w}_{\hat{\mathbf{u}}}^c, d\mathbf{w}_{\hat{\mathbf{v}}}^c, d\mathbf{w}_T^c, d\mathbf{w}_S^c, d\mathbf{w}_\psi^c)^T$
- PE dynamical model operator: $\mathbf{f}^{PE}(\cdot, t)$
- linear extrapolation matrix, from coarse to fine state: $\mathbf{B}^{fc}(t)$

Stochastic Primitive Equation Model

*Internal Baroclinic
Zonal Mode*

$$d\hat{\mathbf{u}} = d\mathbf{u}' - d\bar{\mathbf{u}}', \quad (82a)$$

$$d\mathbf{u}' = \left(-\Gamma(\mathbf{u}) + f\mathbf{v} - \frac{g}{\rho_0} \int_z^0 \rho_x \, dz + \mathbf{F}_u + \mathbf{A}_v \mathbf{u}_{zz} \right) dt + \mathbf{B}_u^{fc} d\tilde{\mathbf{w}}_u^c, \\ \text{with } \mathbf{u} = \hat{\mathbf{u}} - \frac{1}{H} \psi_y.$$

$$d\tilde{\mathbf{w}}_u^c = -\beta_u \tilde{\mathbf{w}}_u^c dt + d\mathbf{w}_u^c, \quad (82b)$$

$$\text{with } \tilde{\mathbf{w}}_u^c(0) \sim (\mathbf{0}, \boldsymbol{\Sigma}_u) \text{ and } \mathbf{w}_u^c \sim (\mathbf{0}, 2\beta_u \boldsymbol{\Sigma}_u).$$

*Internal Baroclinic
Meridional Mode*

$$d\hat{\mathbf{v}} = d\mathbf{v}' - d\bar{\mathbf{v}}', \quad (82c)$$

$$d\mathbf{v}' = \left(-\Gamma(\mathbf{v}) - f\mathbf{u} - \frac{g}{\rho_0} \int_z^0 \rho_y \, dz + \mathbf{F}_v + \mathbf{A}_v \mathbf{v}_{zz} \right) dt + \mathbf{B}_v^{fc} d\tilde{\mathbf{w}}_v^c, \\ \text{with } \mathbf{v} = \hat{\mathbf{v}} + \frac{1}{H} \psi_x.$$

$$d\tilde{\mathbf{w}}_v^c = -\beta_v \tilde{\mathbf{w}}_v^c dt + d\mathbf{w}_v^c, \quad (82d)$$

$$\text{with } \tilde{\mathbf{w}}_v^c(0) \sim (\mathbf{0}, \boldsymbol{\Sigma}_v) \text{ and } \mathbf{w}_v^c \sim (\mathbf{0}, 2\beta_v \boldsymbol{\Sigma}_v).$$

*Thermal energy:
Balance*

$$d\mathbf{T} = \left(-\Gamma(\mathbf{T}) + \mathbf{F}_T + \mathbf{K}_v \mathbf{T}_{zz} \right) dt + \mathbf{B}_T^{fc} d\tilde{\mathbf{w}}_T^c, \quad (82e)$$

$$d\tilde{\mathbf{w}}_T^c = -\beta_T \tilde{\mathbf{w}}_T^c dt + d\mathbf{w}_T^c, \quad (82f)$$

$$\text{with } \tilde{\mathbf{w}}_T^c(0) \sim (\mathbf{0}, \boldsymbol{\Sigma}_T) \text{ and } \mathbf{w}_T^c \sim (\mathbf{0}, 2\beta_T \boldsymbol{\Sigma}_T).$$

*Conservation :
of Salt*

$$d\mathbf{S} = \left(-\Gamma(\mathbf{S}) + \mathbf{F}_S + \mathbf{K}_v \mathbf{S}_{zz} \right) dt + \mathbf{B}_S^{fc} d\tilde{\mathbf{w}}_S^c, \quad (82g)$$

$$d\tilde{\mathbf{w}}_S^c = -\beta_S \tilde{\mathbf{w}}_S^c dt + d\mathbf{w}_S^c, \quad (82h)$$

$$\text{with } \tilde{\mathbf{w}}_S^c(0) \sim (\mathbf{0}, \boldsymbol{\Sigma}_S) \text{ and } \mathbf{w}_S^c \sim (\mathbf{0}, 2\beta_S \boldsymbol{\Sigma}_S).$$

*Barotropic Stream
Function*

$$\nabla_h \wedge [\mathbf{H}^{-1} \nabla_h \wedge d\psi \mathbf{e}_3] = -\nabla_h \wedge d\bar{\mathbf{u}} + \mathbf{B}_\psi^{fc} d\tilde{\mathbf{w}}_\psi^c, \quad (82i)$$

$$d\tilde{\mathbf{w}}_\psi^c = -\beta_\psi \tilde{\mathbf{w}}_\psi^c dt + d\mathbf{w}_\psi^c. \quad (82j)$$

$$\text{with } \tilde{\mathbf{w}}_\psi^c(0) \sim (\mathbf{0}, \boldsymbol{\Sigma}_\psi) \text{ and } \mathbf{w}_\psi^c \sim (\mathbf{0}, 2\beta_\psi \boldsymbol{\Sigma}_\psi).$$

The diagonal of time-decorrelations:

$\beta_u, \beta_v, \beta_T, \beta_S, \beta_\psi$ functions of (x, y, z)

are here chosen $\beta_X = \beta \mathbf{I}$.

**The diagonal of noise variances are chosen
function of z only, of amplitude set to:**

“ ϵ * geostrophy”

$$\boldsymbol{\Sigma}_u = \boldsymbol{\Sigma}_v = \sigma^2(z) \mathbf{I}, \quad \text{with } \sigma_U(z) = \epsilon_U f_c U(z),$$

$$\boldsymbol{\Sigma}_T = \sigma_T^2(z) \mathbf{I}, \quad \text{with } \sigma_T(z) = \epsilon_T U(z) \frac{\Delta T(z)}{L(z)},$$

$$\boldsymbol{\Sigma}_S = \sigma_S^2(z) \mathbf{I}, \quad \text{with } \sigma_S(z) = \epsilon_S U(z) \frac{\Delta S(z)}{L(z)},$$

$$\boldsymbol{\Sigma}_\psi = \sigma_\psi^2(z) \mathbf{I}, \quad \text{with } \sigma_\psi(z) = \epsilon_\psi \frac{\bar{\omega} L(z)}{U(z)},$$

Data-Forecast Melding: Minimum Error Variance within Error Subspace

TRUNCATED Minimum Sample ES Variance, Linear Update (subscript k omitted)

Dynamical State Update: $\hat{\mathbf{x}}(+)=\hat{\mathbf{x}}(-)+\mathbf{K}^p\left(\mathbf{y}^o-\mathcal{H}\left(\hat{\mathbf{x}}(-)\right)\right)$.

Sample ES Optimal Gain: $\mathbf{K}^p=\mathbf{E}_-\mathbf{\Pi}(-)\mathbf{H}^{pT}\left(\mathbf{H}^p\mathbf{\Pi}(-)\mathbf{H}^{pT}+\mathbf{R}\right)^{-1}$, where $\mathbf{H}^p\dot{=} \mathbf{H}\mathbf{E}_-$.

Sample ES Cov. Update: $\mathbf{L}\mathbf{\Pi}(+)\mathbf{L}^T=\mathbf{\Pi}(-)-\mathbf{\Pi}(-)\mathbf{H}^{pT}\left(\mathbf{H}^p\mathbf{\Pi}(-)\mathbf{H}^{pT}+\mathbf{R}\right)^{-1}\mathbf{H}^p\mathbf{\Pi}(-)$.
 $\mathbf{E}_+=\mathbf{E}_-\mathbf{L}$.

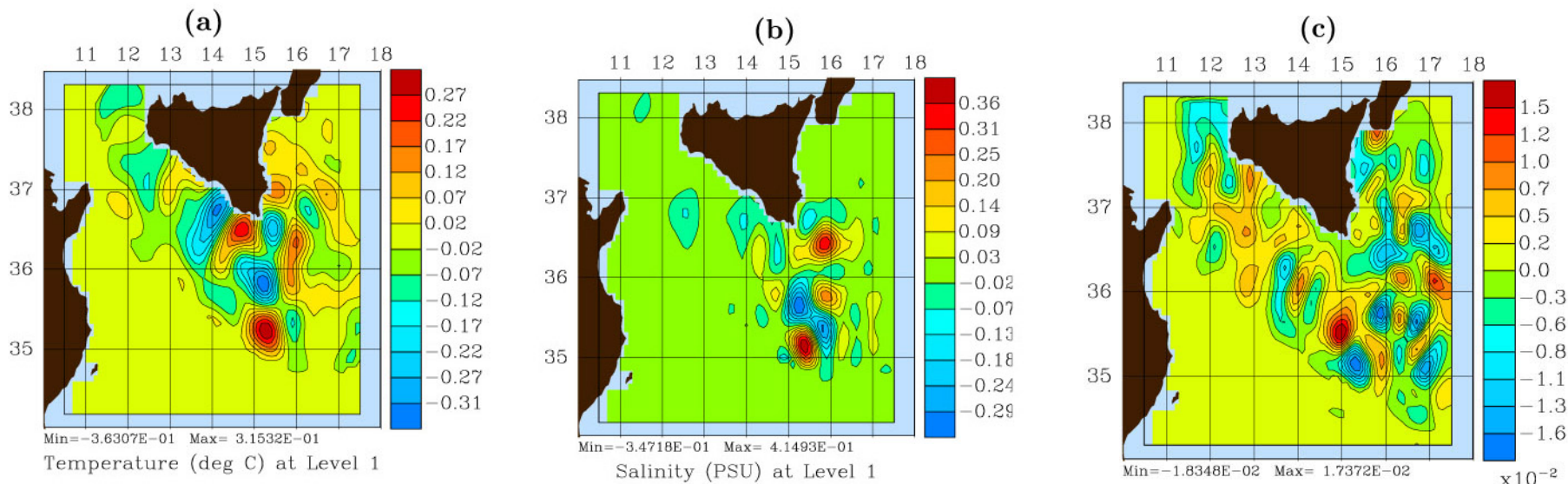
ADAPTIVE LEARNING of the Error Subspace (subscript k omitted)

$\hat{\mathbf{n}}(+)=\mathbf{K}_{\text{trc}}\left(\mathbf{y}^o-\mathcal{H}\left(\hat{\mathbf{x}}(+)\right)\right)$,

$\mathbf{K}_{\text{trc}}=\mathbf{E}_{\text{trc}}(-)\mathbf{\Pi}_{\text{trc}}(-)\mathbf{H}_{\text{trc}}^T\left(\mathbf{H}_{\text{trc}}\mathbf{\Pi}_{\text{trc}}(-)\mathbf{H}_{\text{trc}}^T+\mathbf{R}\right)^{-1}$, where $\mathbf{H}_{\text{trc}}\dot{=} \mathbf{H}\mathbf{E}_{\text{trc}}(-)$.

$\mathbf{E}_+\mathbf{\Sigma}^a(+)\mathbf{V}_+^{aT}=\text{SVD}_{p+1}\left(\left[\mathbf{E}_+\mathbf{\Sigma}(+),\hat{\mathbf{n}}(+)\right]\right)$,

$\mathbf{\Pi}^a(+)=\frac{1}{q+1}\mathbf{\Sigma}^{a2}(+)$.



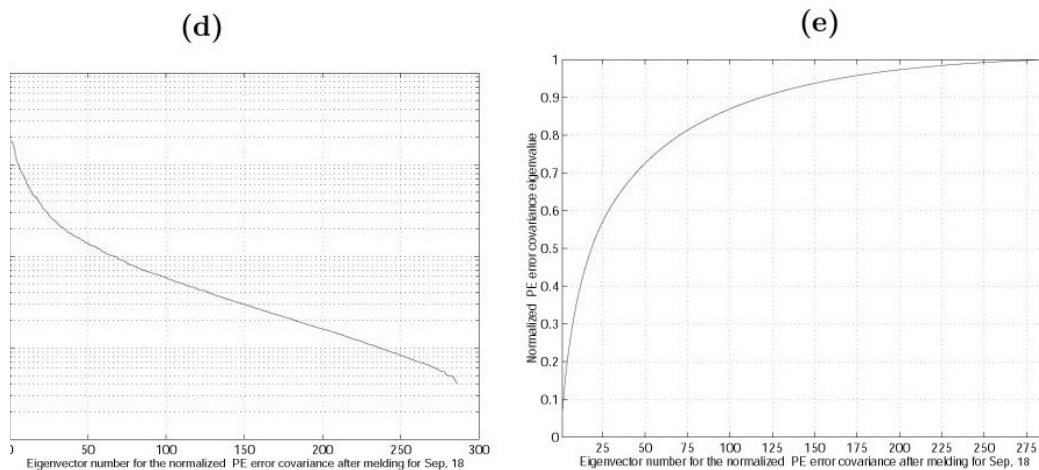
Adaptive learning of dominant errors

Panels (a–b) show the surface T, S gridded *a posteriori* data residuals as estimated by ESSE objective analysis on Sep. 18.

Panel (c) is the surface S of error vector number 81 after adaptation. This vector explains parts of the residual shown by (b).

Panel (d) is the eigenvalue spectrum of the normalized ES covariance after adaptation.

Panel (e) is the cumulative (0-1) spectrum associated with (d). Using 50 vectors explains 73% of the variance explained by the 286 vectors; 100 vectors explain 87% of that variance. Comparing with Fig. 13, the assimilation flattens the error spectrum.

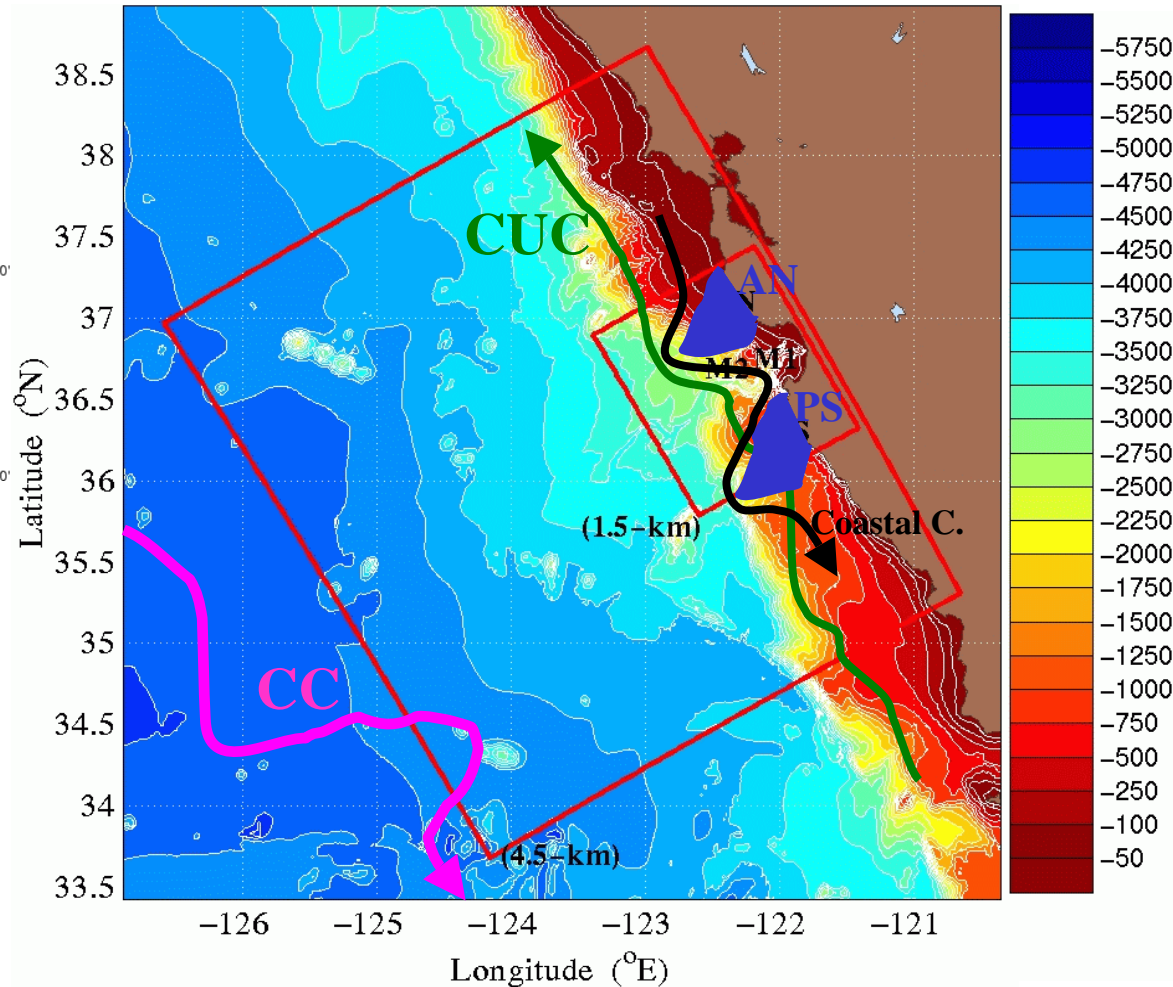
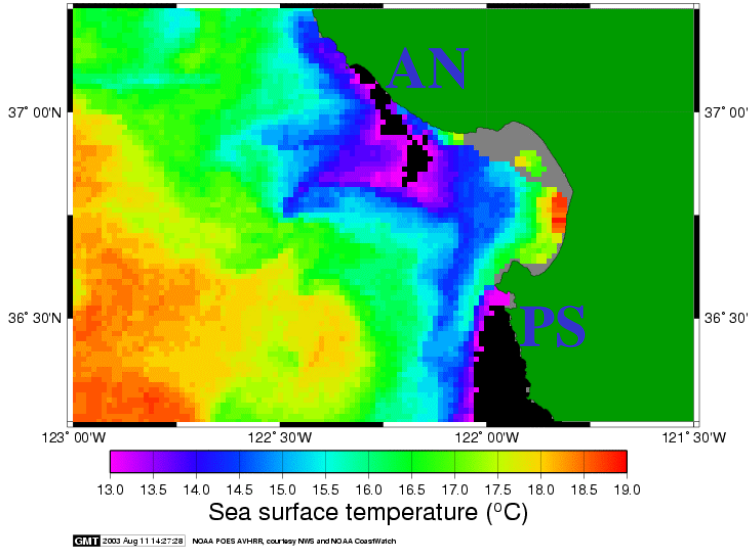


Lermusiaux, DAO (1999)

REGIONAL FEATURES of Monterey Bay and California Current System and Real-time Modeling Domains (AOSN2, 4 Aug. – 3 Sep., 2003)

SST on August 11, 2003

Experimental AVHRR HRPT SST August 11, 2003 1850 h UTC



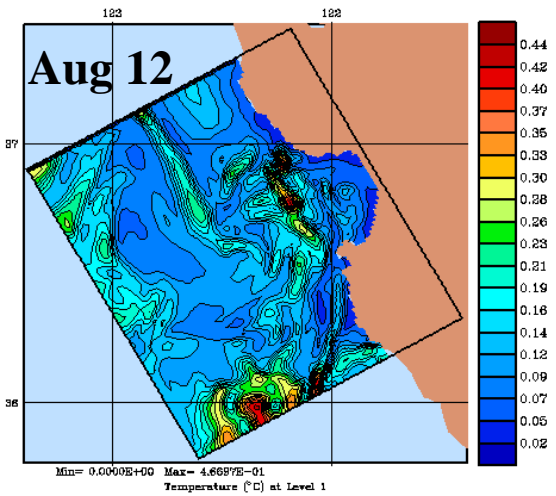
REGIONAL FEATURES

- **Upwelling centers at Pt AN/ Pt Sur:**.....Upwelled water advected equatorward and seaward
- **Coastal current, eddies, squirts, filam., etc:**....Upwelling-induced jets and high (sub)-mesoscale var. in CTZ
- **California Undercurrent (CUC):**.....Poleward flow/jet, 10-100km offshore, 50-300m depth
- **California Current (CC):**.....Broad southward flow, 100-1350km offshore, 0-500m depth

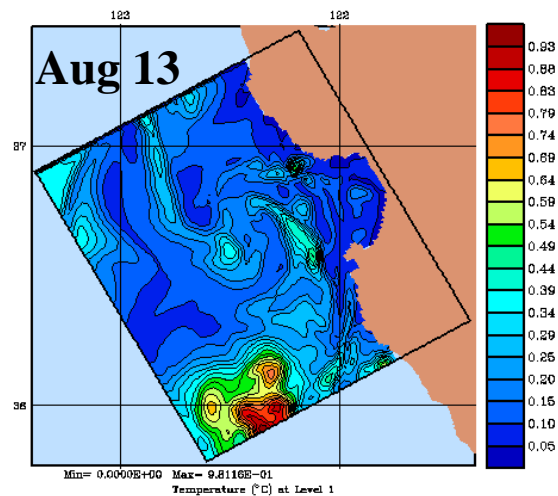
Real-time ESSE : AOSN-II Accomplishments

- 10 sets of ESSE nowcasts and forecasts of temperature, salinity and velocity, and their uncertainties, issued from 4 Aug. to 3 Sep.
 - Total of 4323 ensemble members: 270 – 500 members per day (7×10^5 state var.)
 - ESSE fields included: central forecasts, ensemble means, *a priori* (forecast) errors, *a posteriori* errors, dominant singular vectors and covariance fields
 - 10^4 data points quality controlled and assimilated per day: ship (Pt. Sur, Martin, Pt. Lobos), glider (WHOI and Scripps) and aircraft SST data
- Ensemble of stochastic PE model predictions (HOPS)
 - Deterministic atmospheric forcing: 3km and hourly COAMPS flux predictions
 - Stochastic oceanic/atmos. forcings for: sub-mesoscale eddies, BCs and atmos. fluxes
- ESSE fields formed the basis for daily adaptive sampling recommendations
- Adaptive ocean modeling: BCs and model parameters for transfer of atmos. fluxes calibrated and modified in real-time to adapt to evolving conditions
- ESSE results described and posted on the Web daily
- Real-time research: stochastic error models, coupled physics-biology, tides

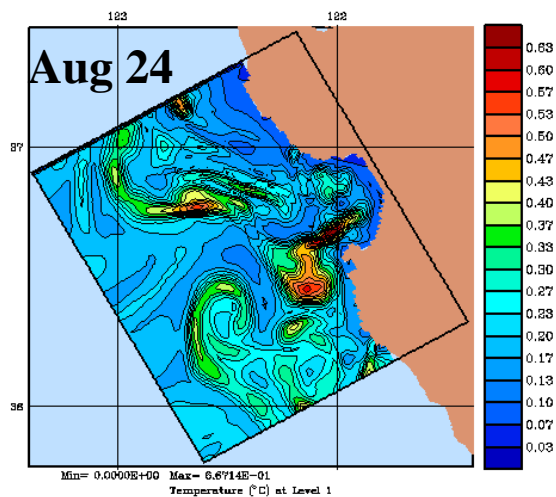
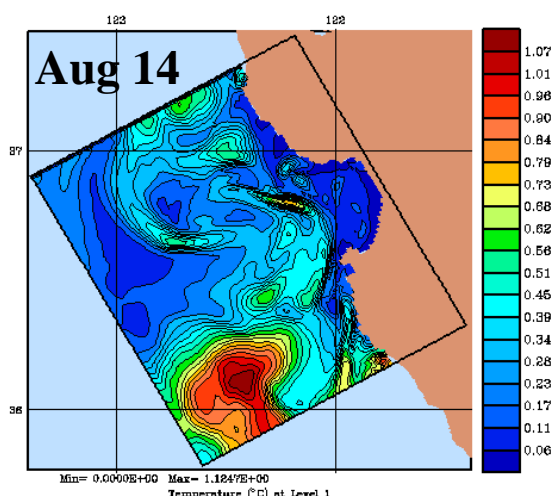
ESSE Surface Temperature Error Standard Deviation Forecasts



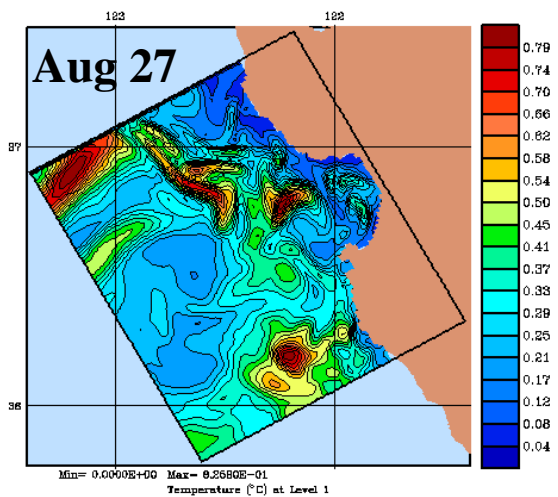
Start of Upwelling



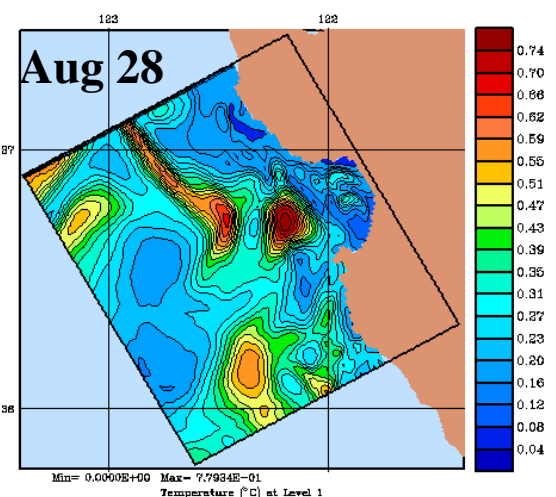
First Upwelling period



End of Relaxation



Second Upwelling period



II. Multiple Facets of Oceanic Adaptive Sampling

Foci	<ul style="list-style-type: none"> - Optimal ocean science (Physics, Acoustics and/or Biology) - Demonstration of adaptive sampling value, etc.
Objective Fields	<ul style="list-style-type: none"> i. Maintain synoptic accuracy (e.g. upwelling, BL or CUC/CCS coverage) ii. Minimize uncertainties (e.g. uncertain ocean estimates), or iii. Maximize the sampling of expected events (e.g. start of upwelling/ relaxation, dynamics of upwelling filament, small scales/model errors) <p>Multidisciplinary or not Local, regional or global, etc.</p>
Time and Space Scales	<ul style="list-style-type: none"> i. Tactical scales (e.g. minutes-to-hours adaptation by each glider) ii. Strategic scales (e.g. hours-to-days adaptation for glider group/cluster) iii. Experiment scales
Assumptions	<ul style="list-style-type: none"> - Fixed or variable environment (w.r.t. asset speeds) - Objective field depends on the predicted data values or not - Operational, time and cost constraints, or not, etc.
Methods	<p>Bayesian-based, Nonlinear programming, (Mixed)-integer programming, Simulated Annealing, Genetic algorithms, Neural networks, Fuzzy logics</p>

For each of the 5 categories, there are multiple choices (only a few listed here)
 Choices set the type of adaptive sampling research

II.a Adaptive sampling via ESSE

- Objective: Minimize predicted trace of full error covariance (T,S,U,V error std Dev).
- Scales: Strategic/Experiment (not tactical yet). Day to week.
- Assumptions: Small number of pre-selected tracks/regions (based on quick look on error forecast and constrained by operation)
- Problem solved: e.g. Compute today, the tracks/regions to sample tomorrow, that will most reduce uncertainties the day after tomorrow.
- Objective field changes during computation and is affected by data to-be-collected
- Model errors Q can account for coverage term

Dynamics: $dx = M(x)dt + d\eta$ $\eta \sim N(0, Q)$

Measurement: $y = H(x) + \varepsilon$ $\varepsilon \sim N(0, R)$

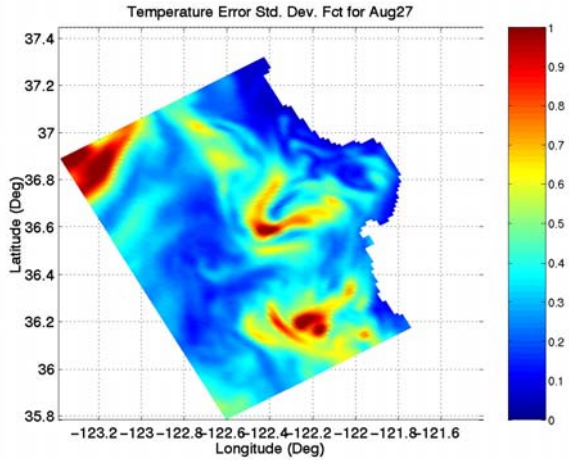
Non-lin. Err. Cov.:

$$dP / dt = \langle (x - \hat{x})(M(x) - M(\hat{x}))^T \rangle + \langle (M(x) - M(\hat{x}))(x - \hat{x})^T \rangle + Q$$

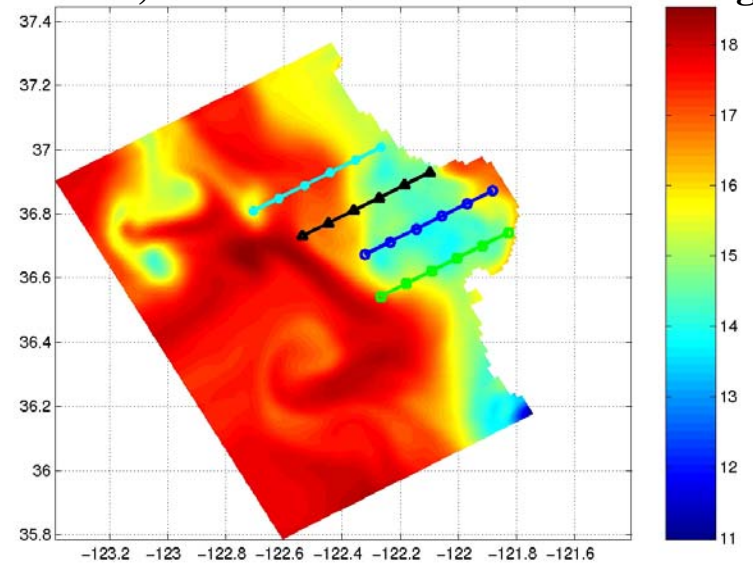
Metric or Cost function: e.g. Find future H_i and R_i such that

$$\underset{H_i, R_i}{Min} \quad tr(P(t_f)) \quad or \quad \underset{H_i, R_i}{Min} \quad \int_{t_0}^{t_f} tr(P(t)) \quad dt$$

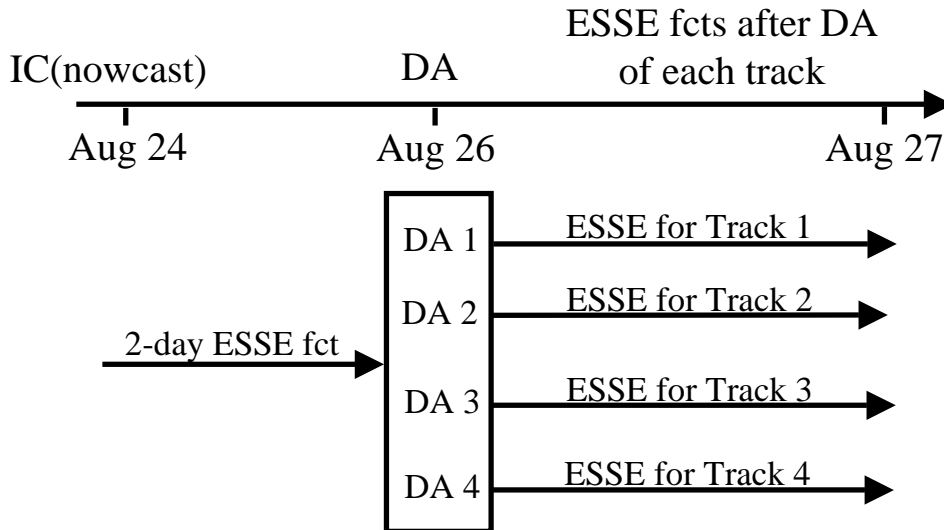
Which sampling on Aug 26 optimally reduces uncertainties on Aug 27?



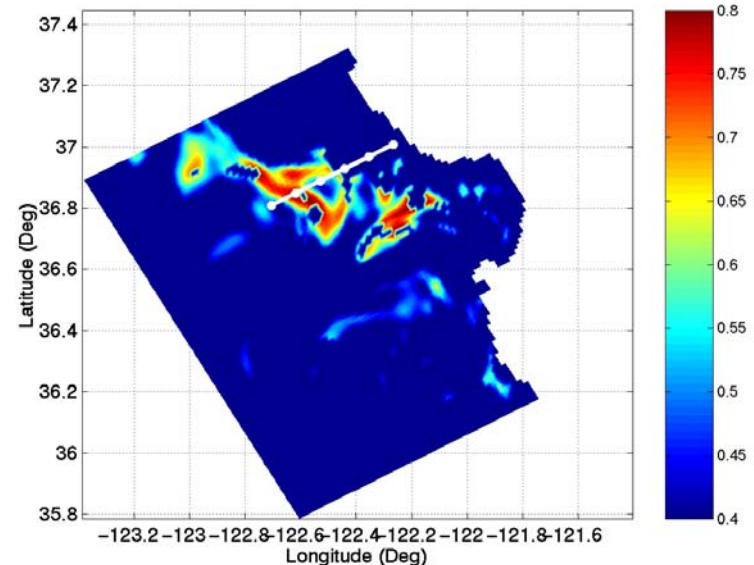
4 candidate tracks, overlaid on surface T fct for Aug 26



- Based on nonlinear error covariance evolution
- For every choice of adaptive strategy, an ensemble is computed



Best predicted relative error reduction: track 1



II.b Optimal Paths Generation for a “fixed” objective field

- Objective: Minimize error standard deviation of temperature field
- Scales: Strategic/Tactical
- Assumptions
 - Speed of platforms \gg time-rate of change of environment
 - Objective field fixed during the computation of the path and is not affected by new data
 - Problem solved: assuming the error is like that now and will remain so for the next few hours, where do I send my gliders/AUVs?
- Methods (global optimization) vary with type of cost function/problem size:
 - *Combinatorial problems*:
 - Objective function is linear or nonlinear, defined over large but finite set of possible solutions (networking, scheduling problems, etc).
 - If cost function piecewise linear, solved *exactly* by Mixed-Integer Programming (MIP)
 - *General unconstrained problems*:
 - Nonlinear function over real numbers with no/simple bounds
 - Partitioning strategies for exact solution, brute force for approx. (simul. annealing, etc)
 - *General constrained problems*:
 - Nonlinear function over real numbers with complex bounds/constraints

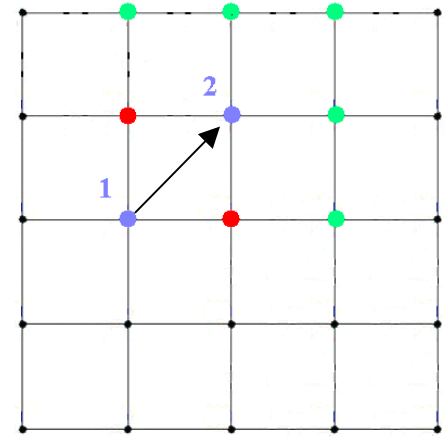
Generation of Paths that minimize ESSE uncertainties using MIP

(Namik K. Yilmaz, P. Lermusiaux and N. Patrikalakis)

- MIP method is often used to solve modified “traveling salesman” problems. Here, towns to be visited are hot-spots in discretized fields and salesmen are the gliders
- Represent ESSE error stand. dev. field as a piecewise-linear cost function
- Possible paths defined on discrete grid: set of possible path is thus finite (but large)

- Constraints on displacements dx , dy , dz :

- No-Return constraints for single vehicle e.g. \Rightarrow
- No-Vicinity constraints for multiple vehicles
- Both can be set by dominant ocean length-scale



- Optimization carried-out by commercial optimization tool Xpress-MP from dash optimization

Example for Two and Three Vehicles, 2D objective field

Two Vehicles

Starting Coordinates:

Vehicle#1:x=37;y=8

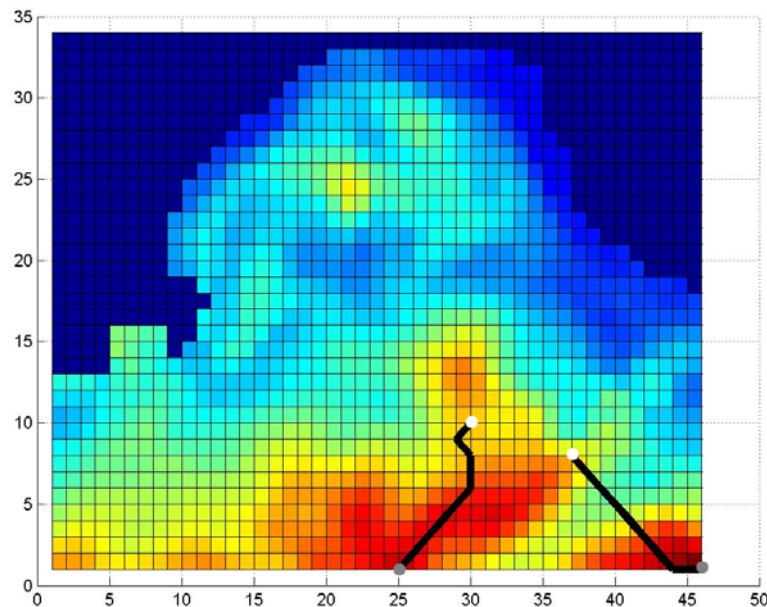
Range1: 19 km

Vehicle#2:x=20;y=10

Range2: 19 km

Total reward: 1185

Vicinity constraint such that two vehicles are away from each other by at least 7 units (11 km).



Three Vehicles

Starting Coordinates:

Vehicle #1 : x=5, y=12

Range=17 km

Vehicle #2 : x=15, y=15

Range=19 km

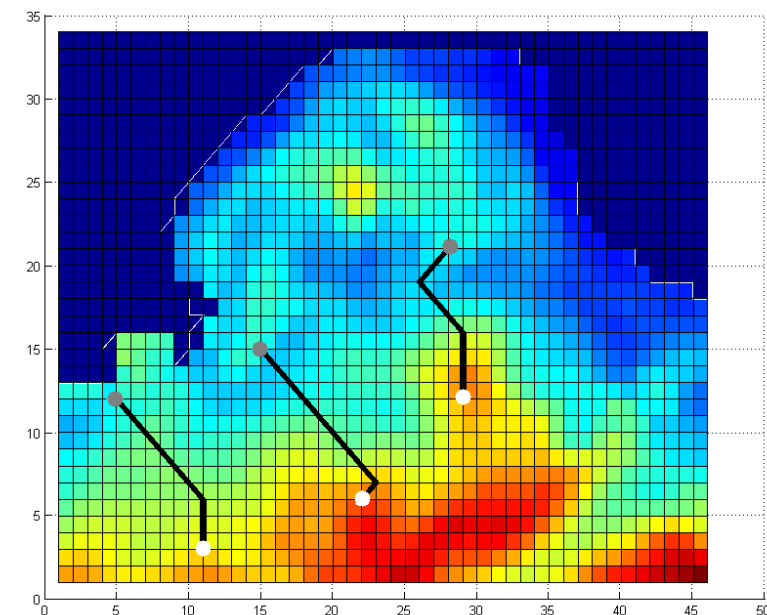
Vehicle #3 : x=28, y=21

Range=17 km

Legend

Grey dots: starting points

White dots: MIP optimal termination points



Example for One Vehicle and 3D objective field

$\forall p \in [1, \dots, P], \text{ and } \forall i \in [2, \dots, N] :$

$$x_{pi} = x_{p(i-1)} + b_{pi1} - b_{pi2}$$

$$b_{pi1} + b_{pi2} \leq 1$$

$$y_{pi} = y_{p(i-1)} + b_{pi3} - b_{pi4}$$

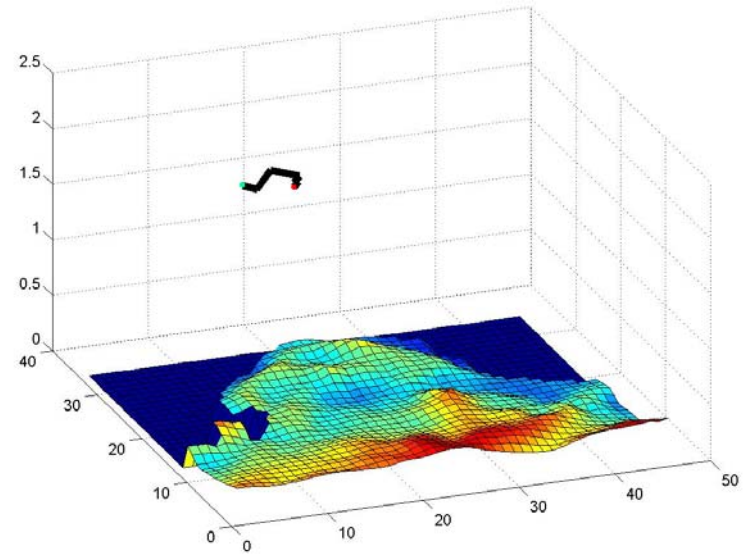
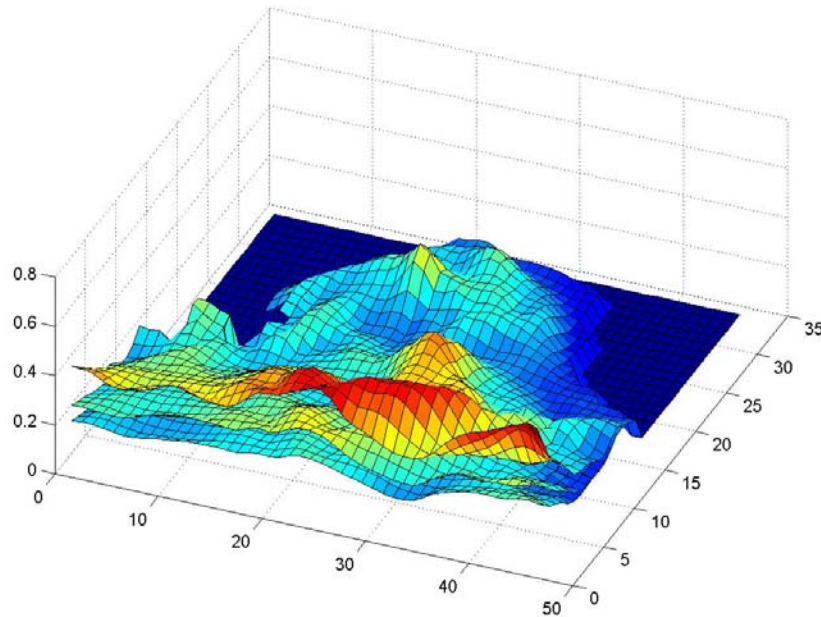
$$b_{pi3} + b_{pi4} \leq 1$$

$$z_{pi} = z_{p(i-1)} + b_{pi5} - b_{pi6}$$

$$b_{pi5} + b_{pi6} \leq 1$$

$\forall p \in [1, \dots, P], \text{ and } \forall i \in [1, \dots, N] :$

$$b_{pi1} + b_{pi2} + b_{pi3} + b_{pi4} \geq 1$$



Starting Coordinates:
 $x=12; y=21$

Range: 10 km

Complete Formulation for 3D Case

N: Number of path points

P: Total number of vehicles

R: Reward matrix designating the 2D data field

$$\max \sum_{p \in [1, \dots, P]} f_{p1} = \sum_{p \in [1, \dots, P]} R[x_{p1}, y_{p1}, z_{p1}]$$

subject to

$$\forall p \in [1, \dots, P], \text{ and } \forall t \in [2, \dots, N] :$$

$$x_{pt} = x_{p(t-1)} + b_{pt1} - b_{pt2}$$

$$b_{pt1} + b_{pt2} \leq 1$$

$$y_{pt} = y_{p(t-1)} + b_{pt3} - b_{pt4}$$

$$b_{pt3} + b_{pt4} \leq 1$$

$$z_{pt} = z_{p(t-1)} + b_{pt5} - b_{pt6}$$

$$b_{pt5} + b_{pt6} \leq 1$$

$$\forall p \in [1, \dots, P], \text{ and } \forall t \in [1, \dots, N] :$$

$$b_{pt1} + b_{pt2} + b_{pt3} + b_{pt4} \geq 1$$

$$\forall p \in [1, \dots, P], \quad \forall t \in [1, \dots, N], \text{ and } \forall j \in [1, \dots, 6] :$$

$$b_{ptj} \in [0, 1]$$

$$\forall p \in [1, \dots, P], \text{ and } \forall t \in [3, \dots, N] :$$

$$x_{pt} - x_{p(t-2)} \geq 2 - M + t1_{pt1}$$

$$x_{p(t-2)} - x_{pt} \geq 2 - M + t1_{pt2}$$

$$y_{pt} - y_{p(t-2)} \geq 2 - M + t1_{pt3}$$

$$y_{p(t-2)} - y_{pt} \geq 2 - M + t1_{pt4}$$

$$z_{pt} - z_{p(t-2)} \geq 2 - M + t1_{pt5}$$

$$z_{p(t-2)} - z_{pt} \geq 2 - M + t1_{pt6}$$

$$t1_{pt1} + t1_{pt2} + t1_{pt3} + t1_{pt4} + t1_{pt5} + t1_{pt6} \leq 5$$

$$\forall p \in [1, \dots, P], \quad \forall t \in [1, \dots, N], \text{ and } \forall j \in [1, \dots, 6] :$$

$$t1_{ptj} \in [0, 1]$$

$$\forall p \in [1, \dots, P], \text{ and } \forall t \in [4, \dots, N] :$$

$$x_{pt} - x_{p(t-3)} \geq 2.5 - M + t2_{pt1}$$

$$x_{p(t-3)} - x_{pt} \geq 2.5 - M + t2_{pt2}$$

$$y_{pt} - y_{p(t-3)} \geq 2.5 - M + t2_{pt3}$$

$$y_{p(t-3)} - y_{pt} \geq 2.5 - M + t2_{pt4}$$

$$z_{pt} - z_{p(t-3)} \geq 2.5 - M + t2_{pt5}$$

$$z_{p(t-3)} - z_{pt} \geq 2.5 - M + t2_{pt6}$$

$$t2_{pt1} + t2_{pt2} + t2_{pt3} + t2_{pt4} + t2_{pt5} + t2_{pt6} \leq 5$$

$$\forall p \in [1, \dots, P], \quad \forall t \in [1, \dots, N], \text{ and } \forall j \in [1, \dots, 6] :$$

$$t2_{ptj} \in [0, 1]$$

$$\forall p \in [1, \dots, P], \text{ and } \forall t \in [5, \dots, N] :$$

$$x_{pt} - x_{p(t-4)} \geq 3 - M + t3_{pt1}$$

$$x_{p(t-4)} - x_{pt} \geq 3 - M + t3_{pt2}$$

$$y_{pt} - y_{p(t-4)} \geq 3 - M + t3_{pt3}$$

$$y_{p(t-4)} - y_{pt} \geq 3 - M + t3_{pt4}$$

$$z_{pt} - z_{p(t-4)} \geq 3 - M + t3_{pt5}$$

$$z_{p(t-4)} - z_{pt} \geq 3 - M + t3_{pt6}$$

$$t3_{pt1} + t3_{pt2} + t3_{pt3} + t3_{pt4} + t3_{pt5} + t3_{pt6} \leq 5$$

$$\forall p \in [1, \dots, P], \quad \forall t \in [1, \dots, N], \text{ and } \forall j \in [1, \dots, 6] :$$

$$t3_{ptj} \in [0, 1]$$

$$\forall p \in [1, \dots, P], \text{ and } \forall q \in [1, \dots, P] : \quad \forall p, q | p > q \text{ and } \forall t, j \in [1, \dots, N] \quad \forall t \in [1, \dots, N] :$$

$$x_{pt} - x_{qt} \geq 2 - M + v1_{pt1}$$

$$x_{qt} - x_{pt} \geq 2 - M + v1_{pt2}$$

$$y_{pt} - y_{qt} \geq 2 - M + v1_{pt3}$$

$$y_{qt} - y_{pt} \geq 2 - M + v1_{pt4}$$

$$z_{pt} - z_{qt} \geq 2 - M + v1_{pt5}$$

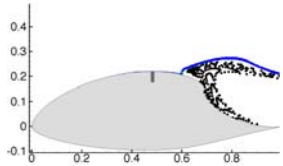
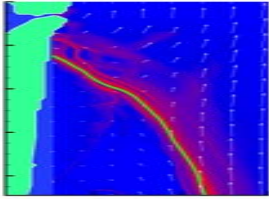
$$z_{qt} - z_{pt} \geq 2 - M + v1_{pt6}$$

$$v1_{pt1} + v1_{pt2} + v1_{pt3} + v1_{pt4} + v1_{pt5} + v1_{pt6} \leq 5$$

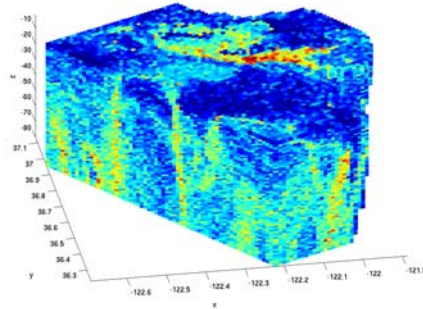
$$\forall p, q \in [1, \dots, P], \quad \forall t \in [1, \dots, N], \text{ and } \forall j \in [1, \dots, 6] :$$

$$v1_{ptj} \in [0, 1]$$

II.c Lagrangian Coherent Structures (LCS): Defined by extrema in direct Lyapunov exponent (scalar field)



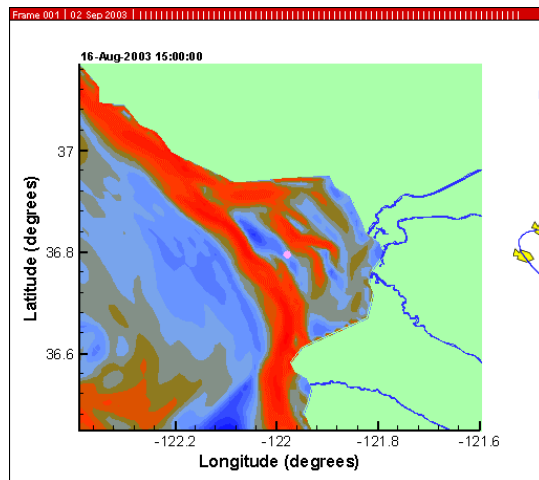
LCS are barriers
in many flows



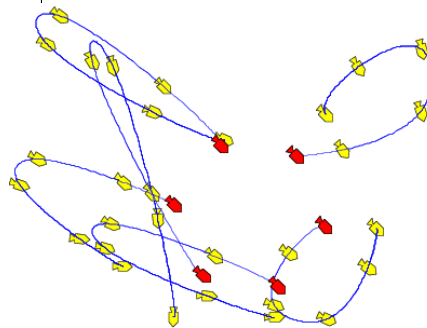
3D capabilities
being developed

Objectives:

- Extend LCS capabilities to 3D
- Relate to biological and geophysical features (temperature fronts, plankton plumes)
- Use LCS for optimal path-planning of underwater gliders (single and groups—deployment and transit)
- Optimization tools for Princeton error metric



Optimal path
lies on an LCS



Optimize group
deployment

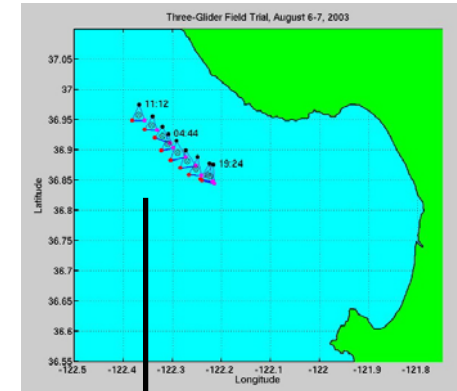
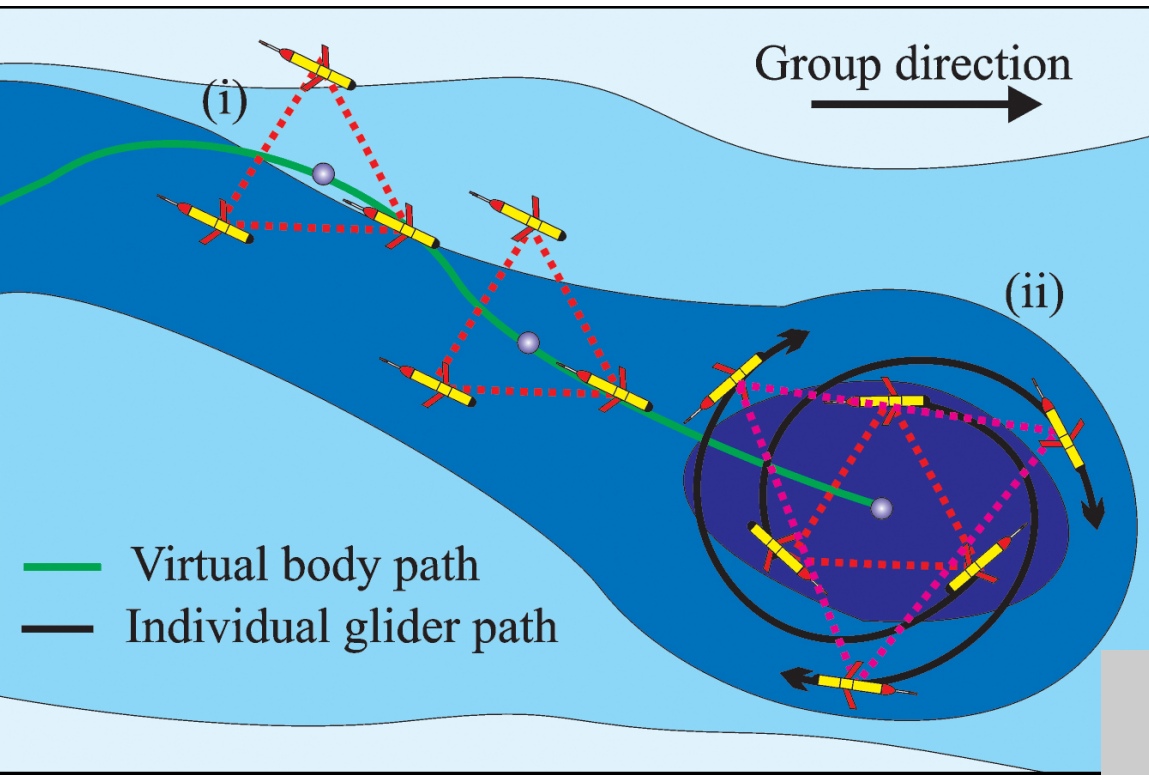
Approach:

- Compute LCS from Observational and Model Predicted oceanographic flow data
- New theory and flux estimates shows precisely how LCS act as barriers
- Use Mangen or GAIO for LCS computations and NTG or DMOC for optimization.

Principal Investigator:

Prof. Jerrold E. Marsden
Dept. of Control and Dynamical Systems
California Institute of Technology

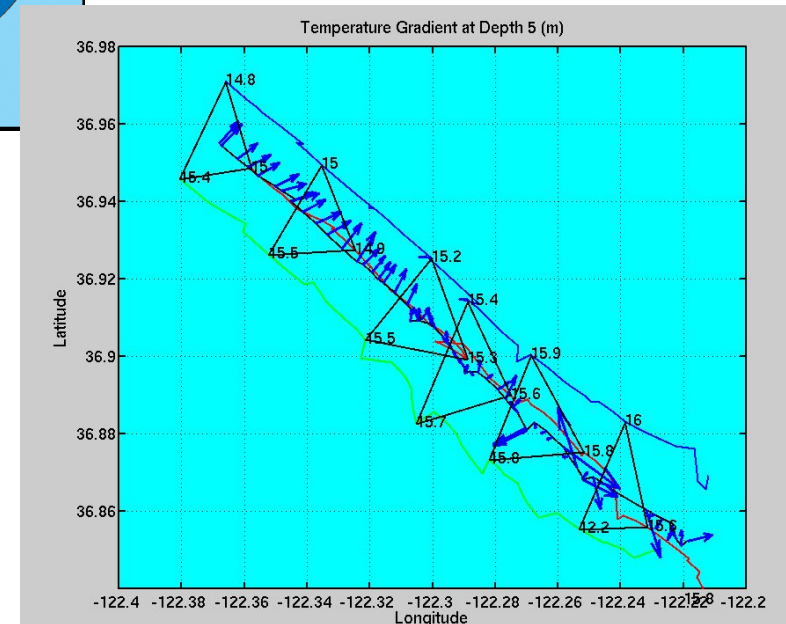
II.d Vehicle Networks for Adaptive Sampling in AOSN-II



Aug 7, 2003

Coordinated 3-Glider Experiment

Three WHOI gliders were coordinated to form an equilateral triangle with side length 3 km and variable orientation angle.



II.e Objective Fields: Flux Balances and/or Term-by-term Balances

- Physical model: Primitive-Equation (PDE, x, y, z, t : HOPS)

Horiz. Mom. $\frac{D\mathbf{u}_h}{Dt} + f \mathbf{e}_3 \wedge \mathbf{u}_h = -\frac{1}{\rho_0} \nabla_h p_w + \nabla_h \cdot (A_h \nabla_h \mathbf{u}_h) + \frac{\partial A_v}{\partial z} \frac{\partial \mathbf{u}_h}{\partial z}$

Vert. Mom. $\rho g + \frac{\partial p_w}{\partial z} = 0$

Thermal en. $\frac{DT}{Dt} = \nabla_h \cdot (K_h \nabla_h T) + \frac{\partial K_v}{\partial z} \frac{\partial T}{\partial z}$

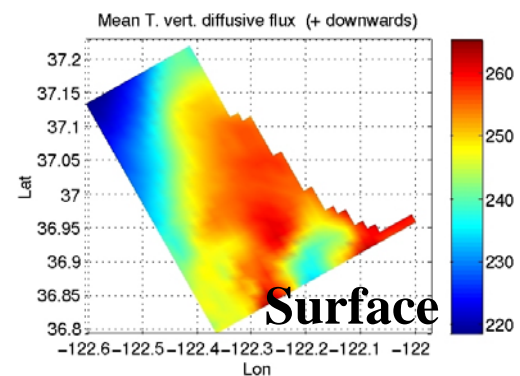
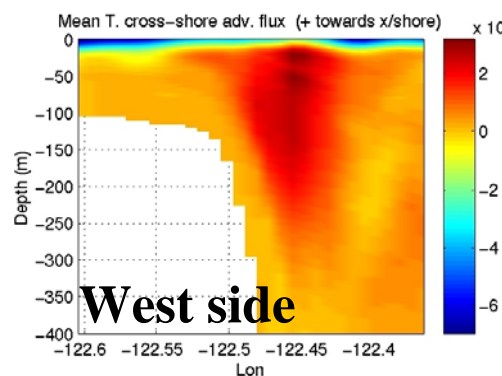
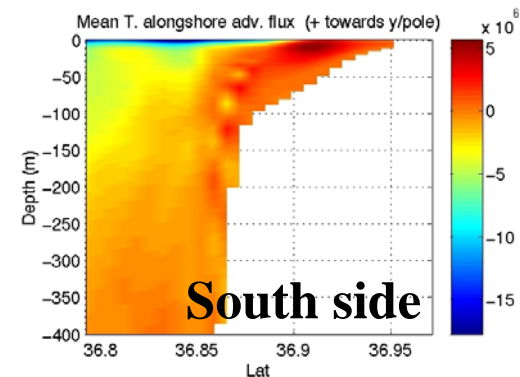
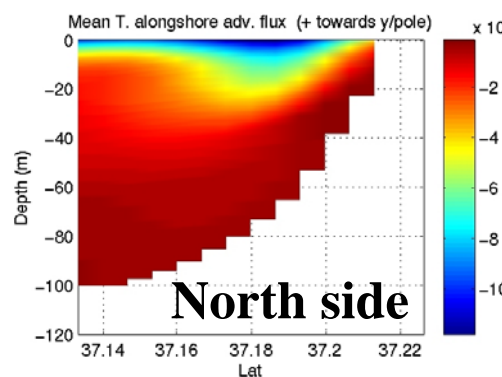
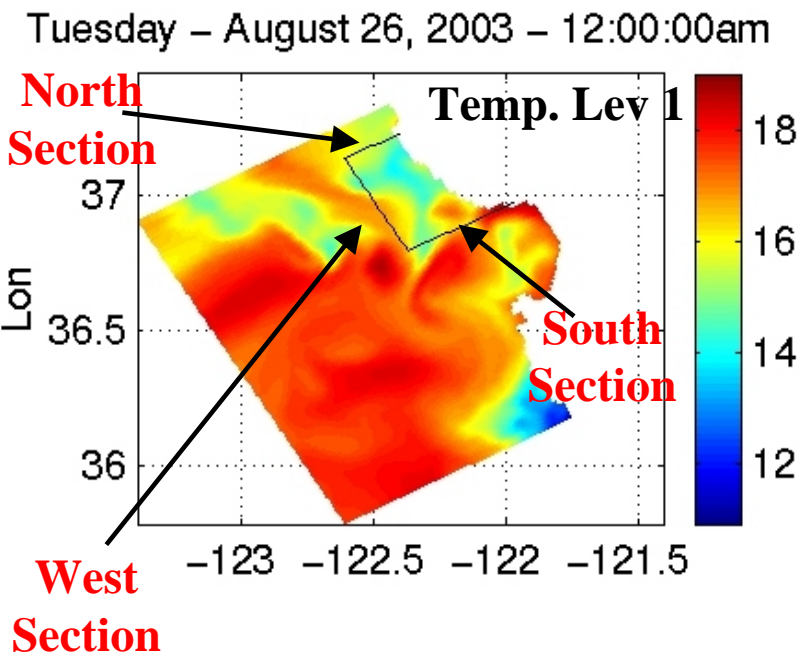
Cons. of salt $\frac{DS}{Dt} = \nabla_h \cdot (K_h \nabla_h S) + \frac{\partial K_v}{\partial z} \frac{\partial S}{\partial z}$

Cons. of mass $\nabla \cdot \mathbf{u} = 0$

Eqn. of state $\rho(\mathbf{r}, z, t) = \rho(T, S, p_w)$

Heat Flux Balances: 4 fluxes normal to each side

Mean Fluxes (W/m²) over: August 6, 2003 – 10:30:00pm → August 13, 2003 – 4:30:00am GMT

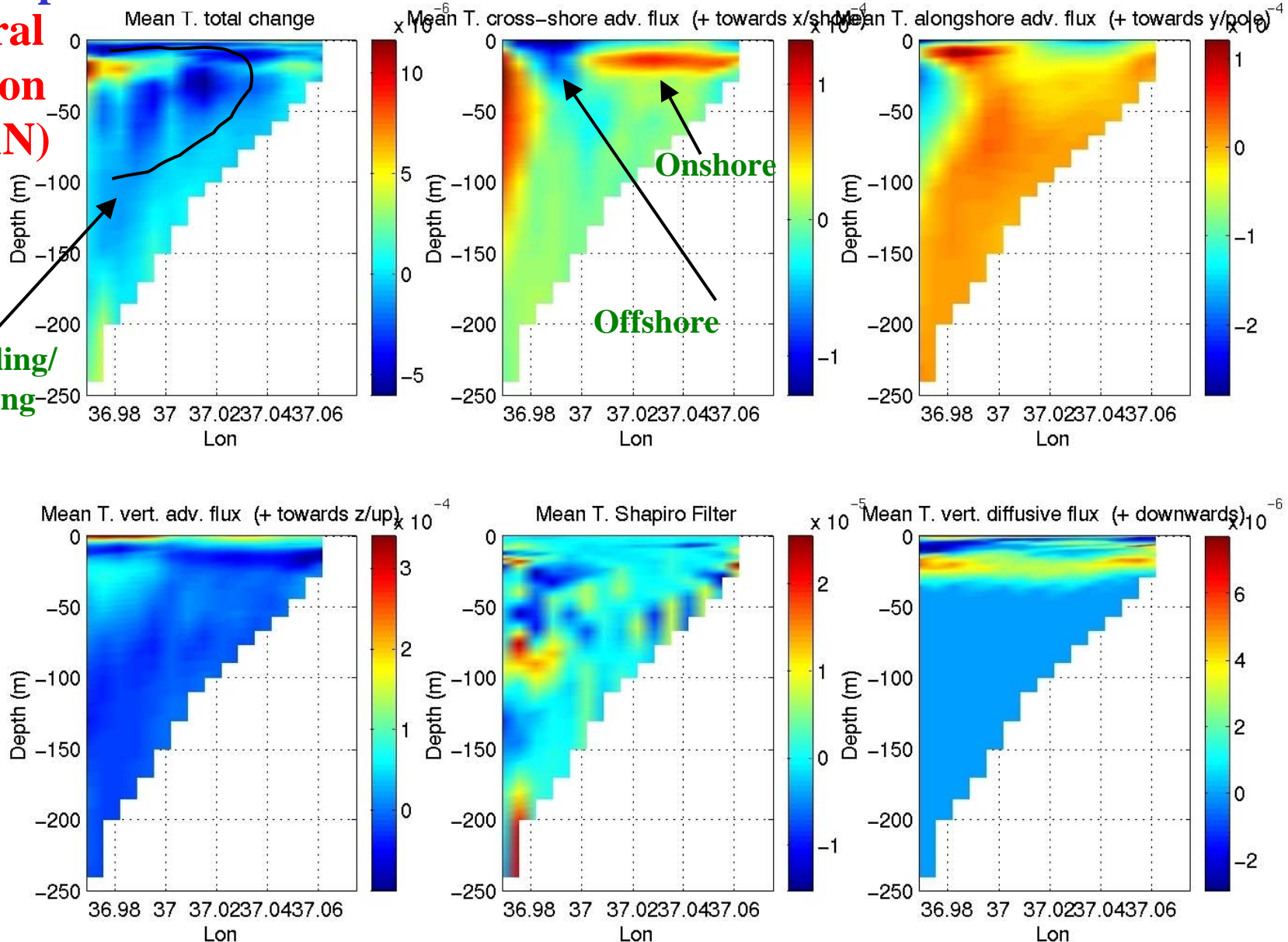


Mean Term-by-Term over: August 6, 2003 – 10:30:00pm → August 17, 2003 – 1:30:00am GMT

Temp. balances

Central
Section
(Pt AN)

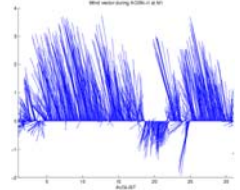
Upwelling/
Cooling



Mean Rate of change \approx (Cross-shore + Alongshore + Vertical) Advection

II.f Objective Field: Multi-Scale Energy and Vorticity Analysis

Two-scale window decomposition in space and time of energy eqns: 11-27 August 2003

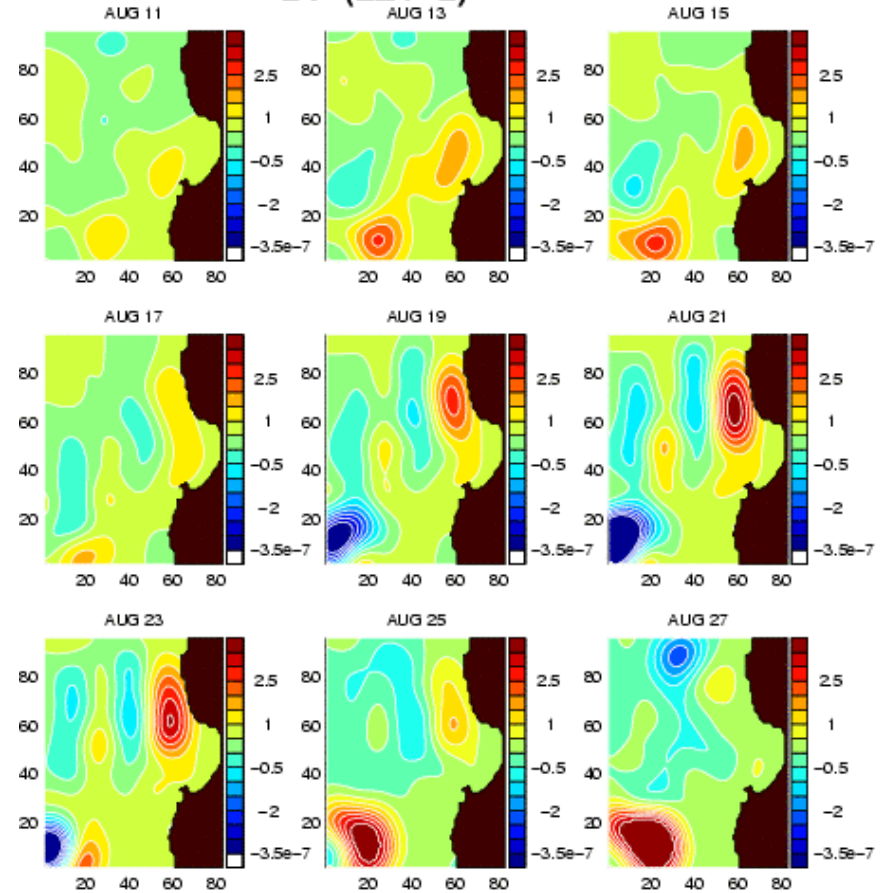
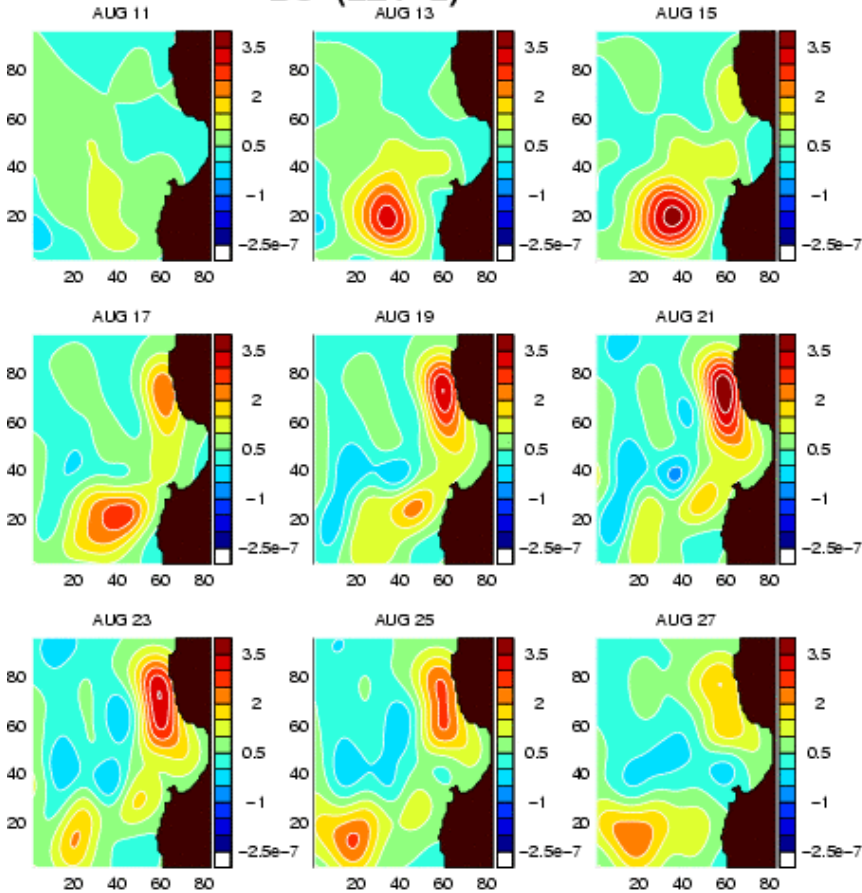


Transfer of APE from large-scale to meso-scale

Transfer of KE from large-scale to meso-scale

BC (LEV=2)

BT (LEV=2)



- Center west of Pt. Sur: winds destabilize the ocean directly.
- Center near the Bay: winds enter the balance on the large-scale window and release energy to the meso-scale window during relaxation.

III.a Forecast Error Analyses and Optimal (Multi) Model Estimates

- Forecast Error Analyses: *Learn individual model forecast errors in an on-line fashion from model-data misfits based on Maximum-Likelihood*
- Model Fusion: *Combine models via Maximum-Likelihood based on the current estimates of their forecast errors*

3-steps strategy, using model-data misfits and error parameter estimation

1. Select appropriate/convenient forecast error parameterization
 - Approximate forecast error covariances and biases models as efficient parametric family:

$$\mathbf{B} \approx \tilde{\mathbf{B}}(\boldsymbol{\alpha}); \quad \boldsymbol{\mu} \approx \tilde{\boldsymbol{\mu}}(\boldsymbol{\beta});$$

- Limit number of free parameters $\boldsymbol{\alpha}$ and $\boldsymbol{\beta}$ (*for now: error length scale and variance*)
2. Adaptively determine forecast error parameters from model-data misfits based on the Maximum-Likelihood principle:

$$\Theta^* = \arg \max_{\Theta} p(\mathbf{y}|\Theta) \quad \mathbf{y} \text{ is the data, } \Theta \text{ the vector of } \boldsymbol{\alpha}'\text{s and } \boldsymbol{\beta}'\text{s of each model}$$

3. Combine model forecasts via Maximum-Likelihood based on the current estimates of error parameters

Forecast Error Analyses and Optimal (Multi) Model Estimates

Forecast Error Parameterization

Limited validation data motivates use of few free parameters

- Approximate forecast error covariances and biases as some parametric family, e.g. homogeneous covariance model:

$$\mathbf{B}_m(i, j) = \sigma(\mathbf{x}_i)\sigma(\mathbf{x}_j)\rho(\|\mathbf{x}_i - \mathbf{x}_j\|); \quad \rho(r) = \exp\left(\frac{-r^2}{2L^2}\right)$$

- Choice of covariance and bias models $\tilde{\mathbf{B}}$ and $\tilde{\boldsymbol{\mu}}$ should be sensible and efficient in terms of $\tilde{\mathbf{B}}\mathbf{v}$, $\tilde{\mathbf{B}}^{-1}\mathbf{v}$ and storage
 - * functional forms (positive semi-definite), e.g. isotropic
 - facilitates use of Recursive Filters and Toeplitz inversion
 - * feature model based
 - sensible with few parameters. Needs more research.
 - * based on dominant error subspaces
 - needs ensemble suite

Forecast Error Analyses and Optimal (Multi) Model Estimates

Error Parameter Tuning

Learn error parameters in an on-line fashion from model-data misfits based on Maximum-Likelihood

- We estimate error parameters via Maximum-Likelihood by solving the problem:

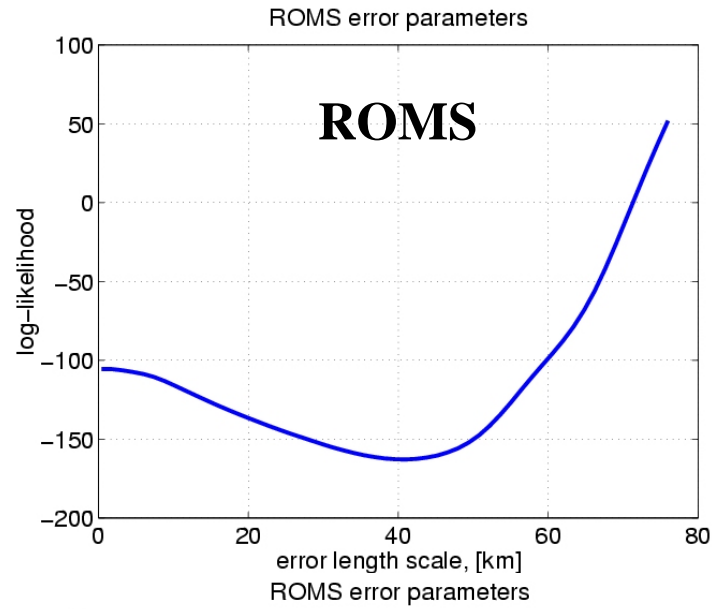
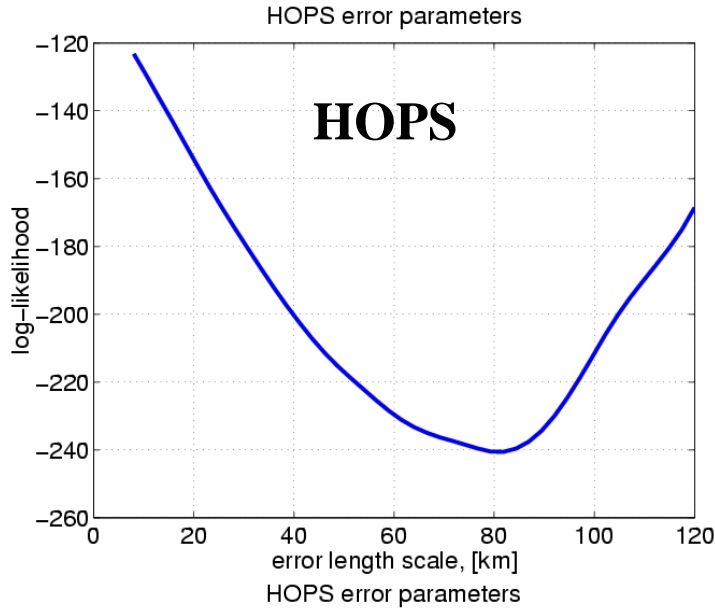
$$\Theta^* = \arg \max_{\Theta} p(\mathcal{Y}|\Theta) \quad (1)$$

Where $\mathcal{Y} = \{\mathbf{y}_1^o, \mathbf{y}_2^o, \dots, \mathbf{y}_T^o\}$ is the observational data, $\Theta = \{\theta_1, \theta_2, \dots, \theta_M\}$ are the forecast error covariance parameters of the M models

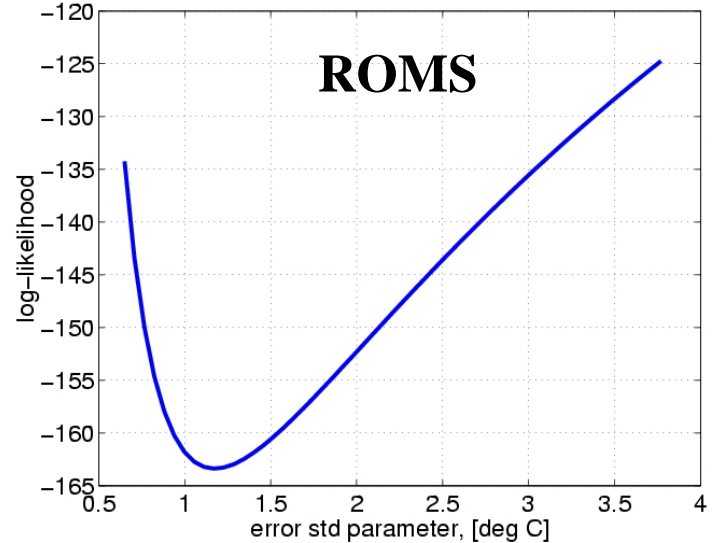
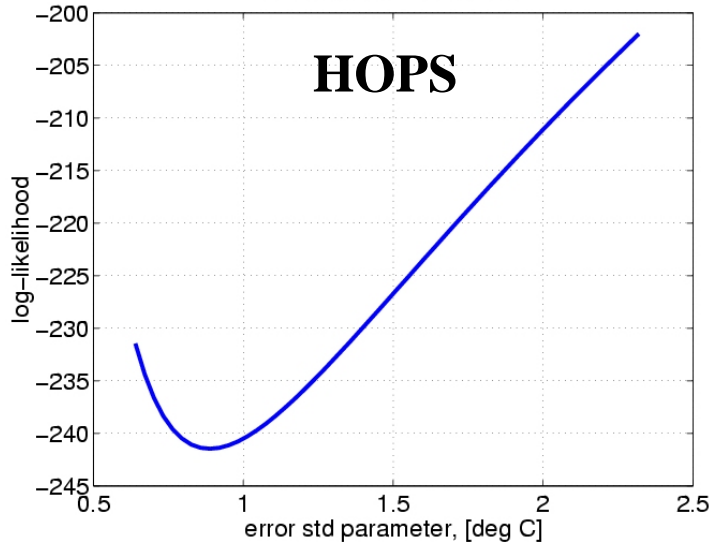
- (1) implies finding parameter values that maximize the probability of observing the data that was, in fact, observed
- By employing a randomized algorithm, we solve (1) relatively efficiently

Forecast Error Analyses and Optimal (Multi) Model Estimates

Log-Likelihood functions for error parameters



**Length
Scale**



Variance

Forecast Error Analyses and Optimal (Multi) Model Estimates

Model Fusion

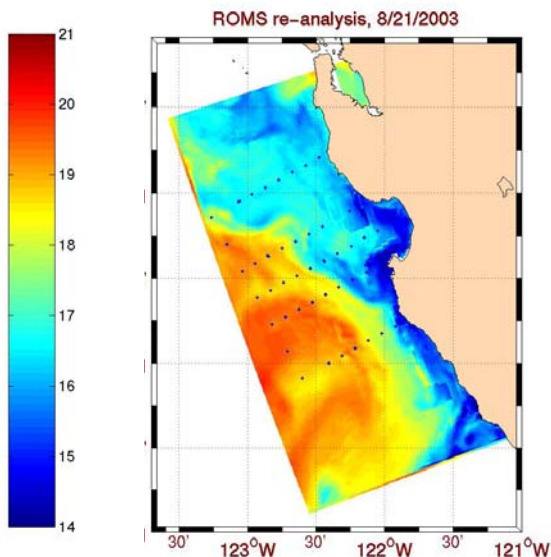
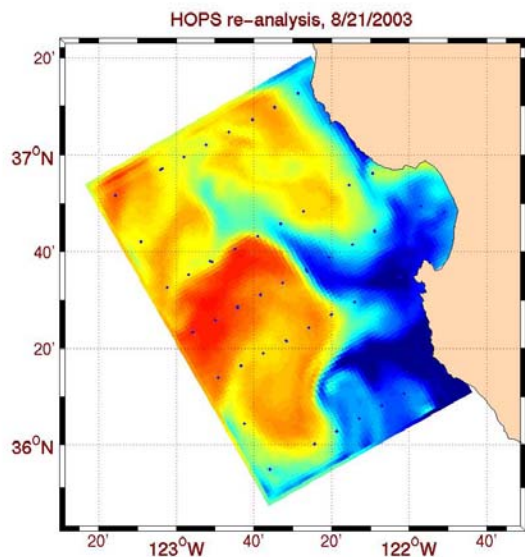
combine based on relative model forecast uncertainties

- **Model Fusion:** once error parameters Θ^* are available, combine forecasts \mathbf{X}_m based on their relative uncertainties as:

$$\mathbf{x}^* = \arg \min_{\mathbf{x}} \sum_{m=1}^M (\mathbf{x} - \mathbf{H}_m \mathbf{x}_m)^T \mathcal{B}_{(\Theta_m)}^{-1} (\mathbf{x} - \mathbf{H}_m \mathbf{x}_m)$$

Forecast Error Analyses and Optimal (Multi) Model Estimates

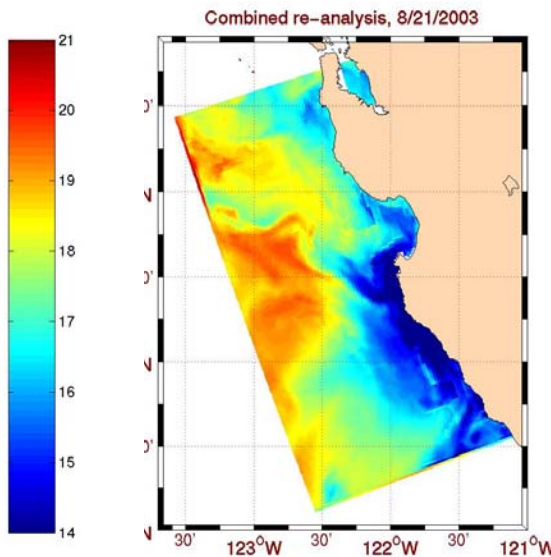
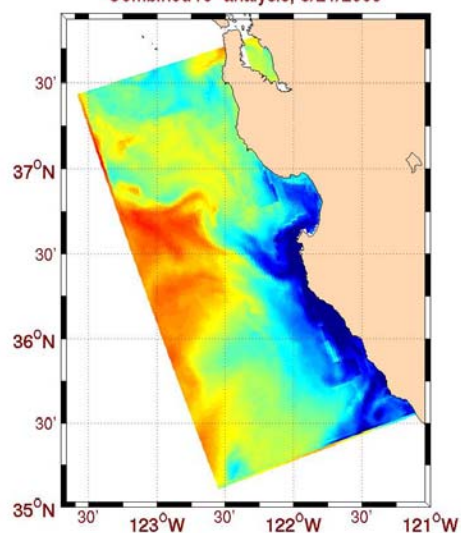
Two-Model Forecasting Example



HOPS and ROMS SST forecast

Left – HOPS
(re-analysis)

Right – ROMS
(re-analysis)



Combined SST forecast

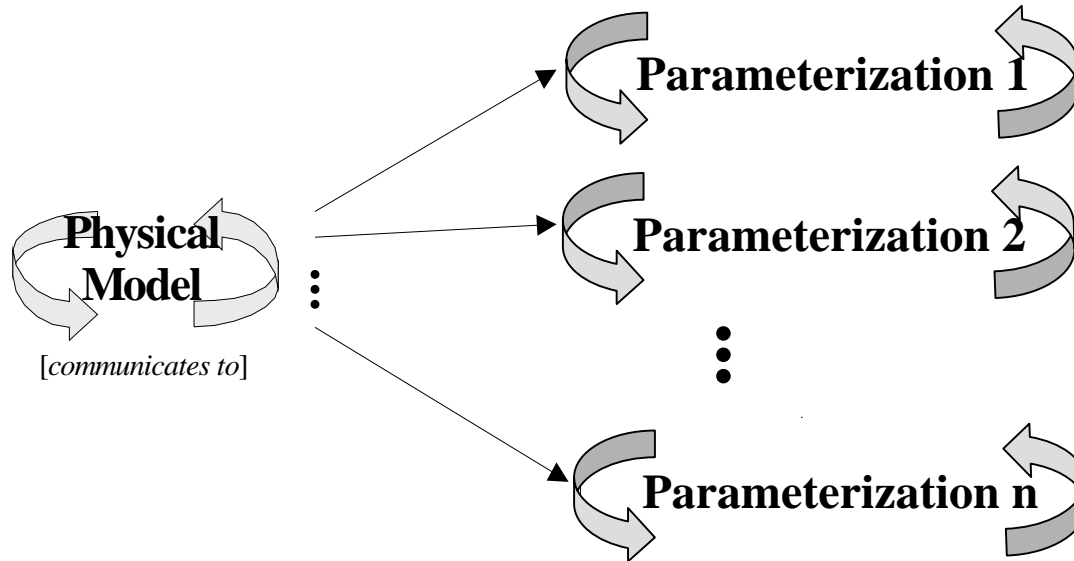
Left – with *a priori*
error parameters

Right – with
Maximum-
Likelihood error
parameters

III.b Oceanic Adaptive Modeling: Motivations and Concepts

- Physical and biogeochemical ocean dynamics can be intermittent and highly variable, and can involve interactions on multiple scales
- In general, oceanic fields and interactions that matter vary in time and space
- Model uncertainties can be (very) large, especially for biogeochemical processes
- For efficient forecasting, model structures and parameters should evolve and respond dynamically to new data injected into the executing prediction system
 - Correction of model biases
 - Comparison of competing models and better scientific understanding
 - Multi-model data assimilation
 - Automated evolution of model structures as a function of model-data misfits
- A model quantity (parameters, structures, state-variables) is said to be adaptive if its formulation, classically assumed constant, is made a function of data values
 - Physical regime transition (e.g., well-mixed to stratified) and evolving/unknown turbulent mixing parameterizations
 - Variations of biological assemblages with time and space (e.g., variable zooplankton dynamics, summer to fall phytoplankton populations, etc) and evolving biogeochemical rates and ratios

Towards Real-time Physical Adaptive Models



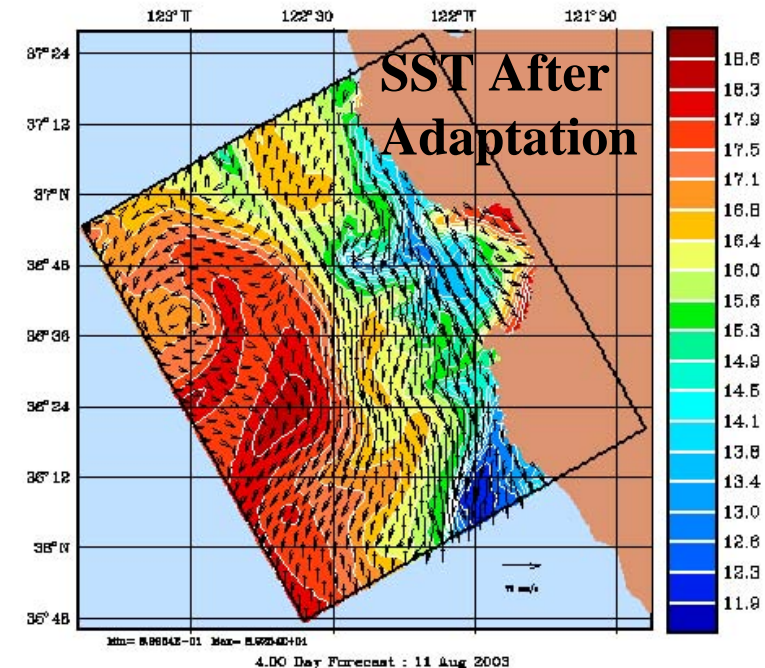
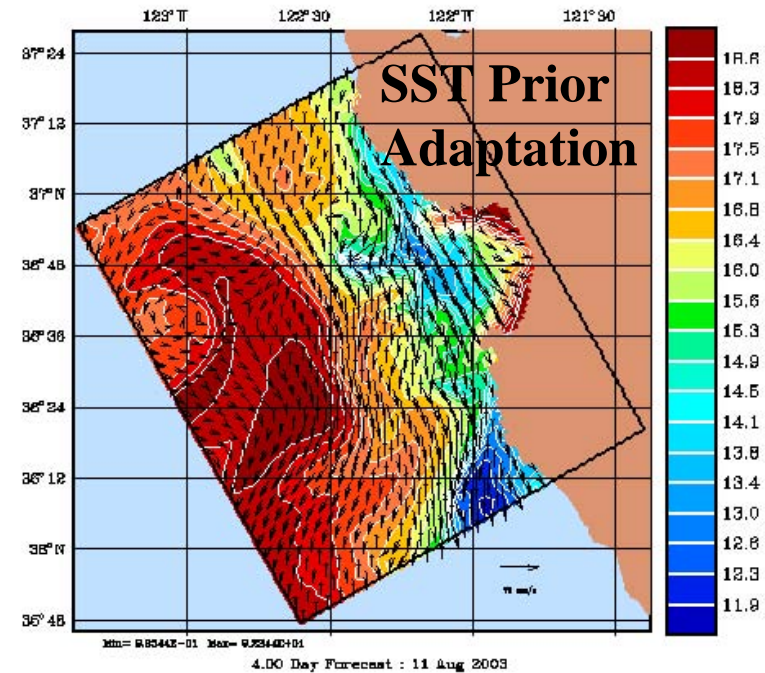
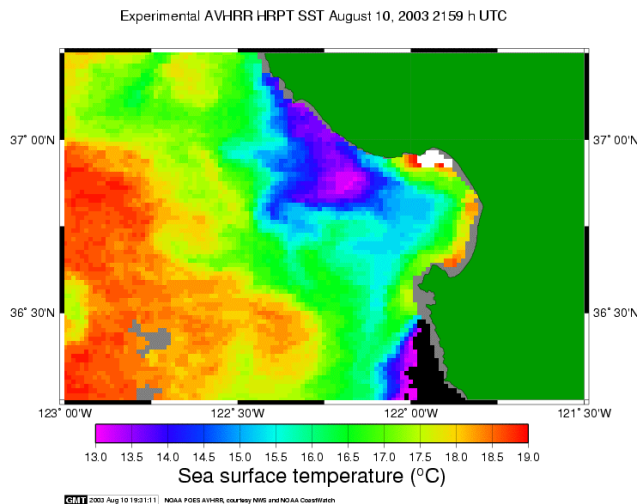
- Different Types of Adaptation:
 - Physical model with multiple parameterizations in parallel (hypothesis testing)
 - Physical model with a single adaptive parameterization (adaptive evolution)
- Model selection based on quantitative dynamical/statistical study of data-model misfits

Quasi-Automated Real-time Physical Calibration during AOSN2

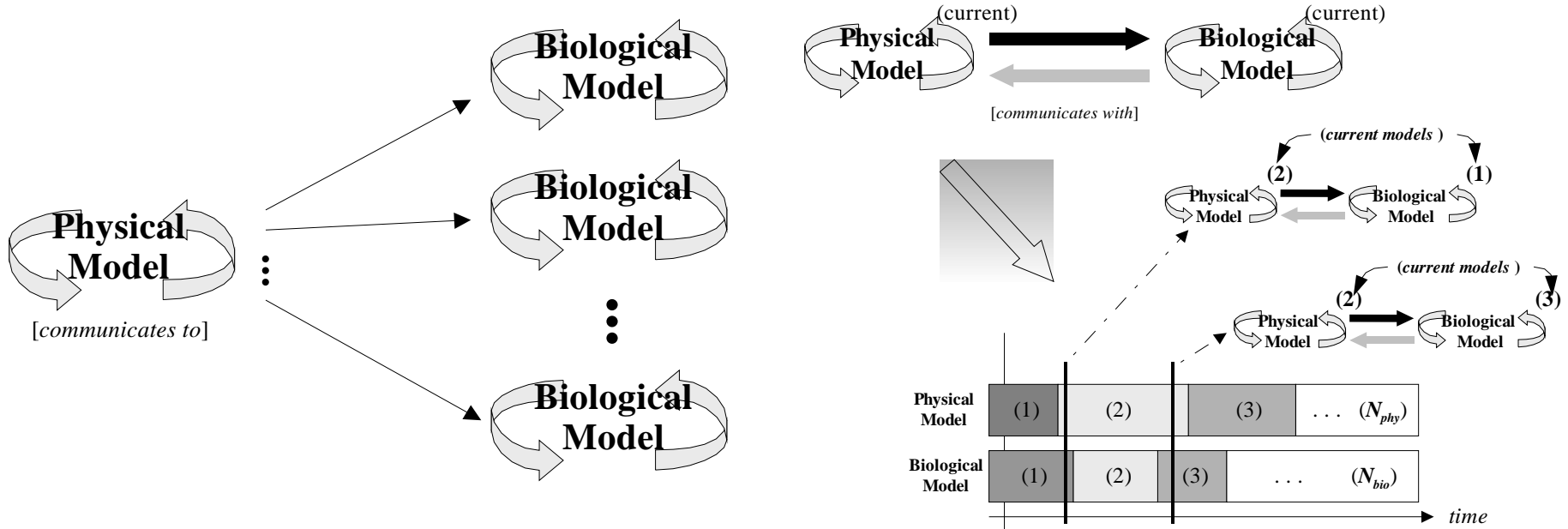
Prior to AOSN2, ocean models calibrated to historical conditions judged to be similar to these expected in August 2003.

Ten days in the experiment:

- Parameterization of the transfer of atmos. fluxes to upper layers (SBL mixing) adapted to new 2003 data
- 20 sets of parameter values and 2 mixing models tested
- Configuration with smallest RMSE/higher PCC improved upper-layer T and S fields, and currents

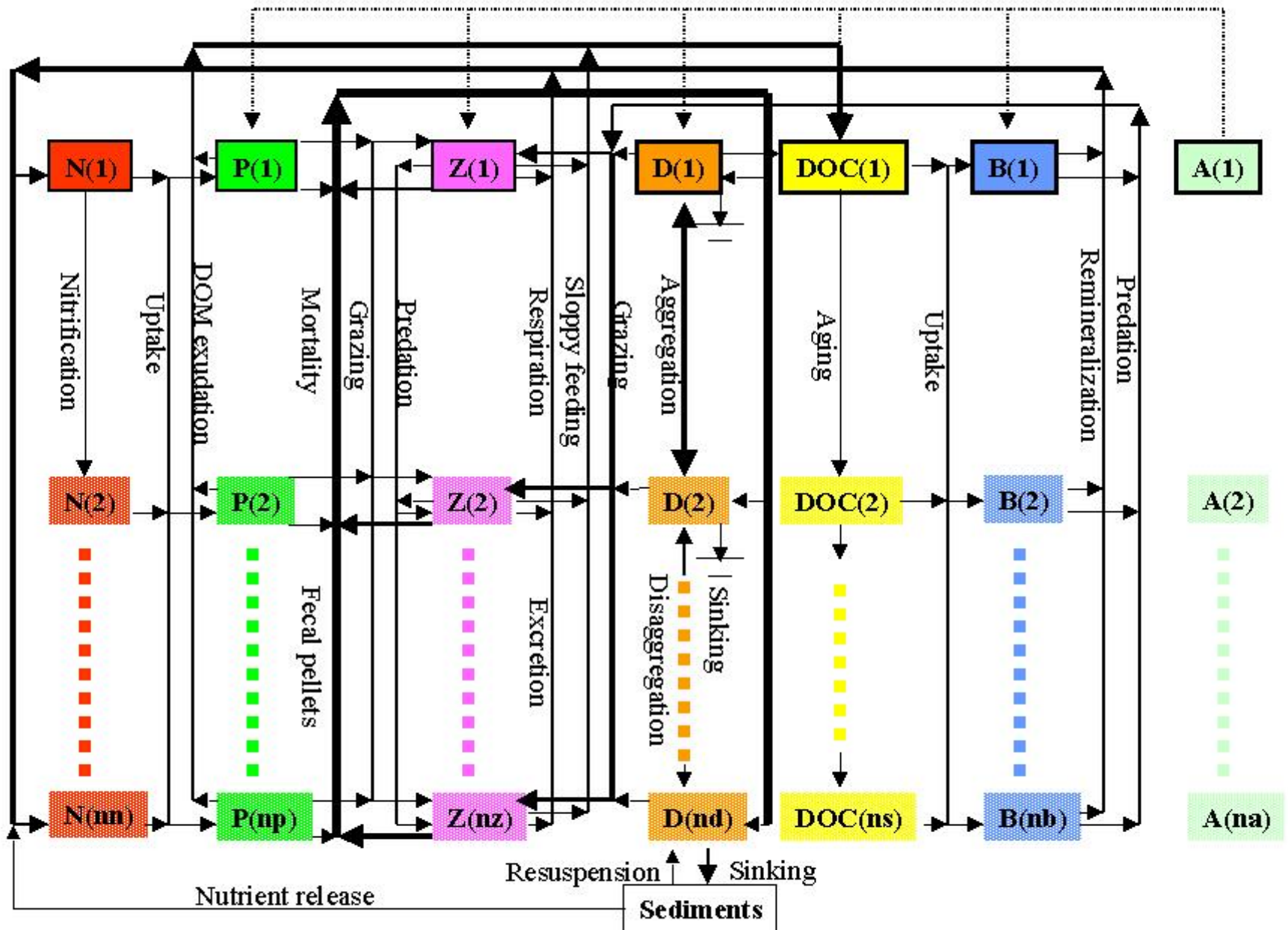


Towards Real-time Adaptive Coupled Models

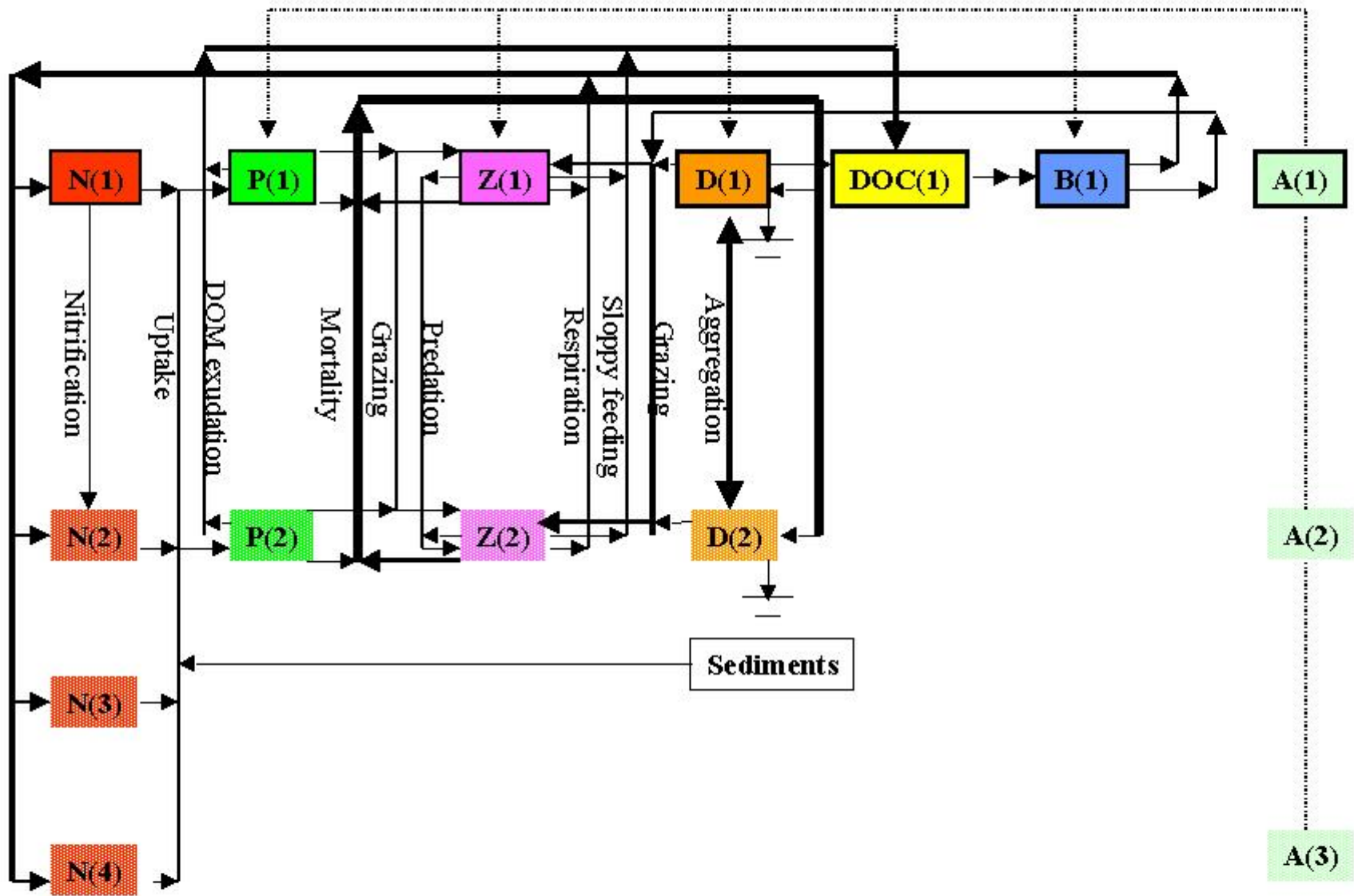


- Different Types of Adaptive Couplings:
 - Adaptive physical model drives multiple biological models (biology hypothesis testing)
 - Adaptive physical model and adaptive biological model proceed in parallel, with some independent adaptation
- Ongoing and Future Numerical Implementation
 - For performance and scientific reasons, both modes are being implemented using message passing for parallel execution
 - Mixed language programming (using C function pointers and wrappers for functional choices)

Generalized Adaptable Biological Model



A Priori Biological Model



Example: Use P data to select parameterizations of Z grazing

Table 1. Parameterization of grazing on multiple types of prey with passive selection (g_{max} : maximum grazing rate; K: Half-saturation constant (but saturation constant in Eq. 1); P_0 threshold below which grazing is zero; p_i : preference coefficient; $?$, a , τ : constant).

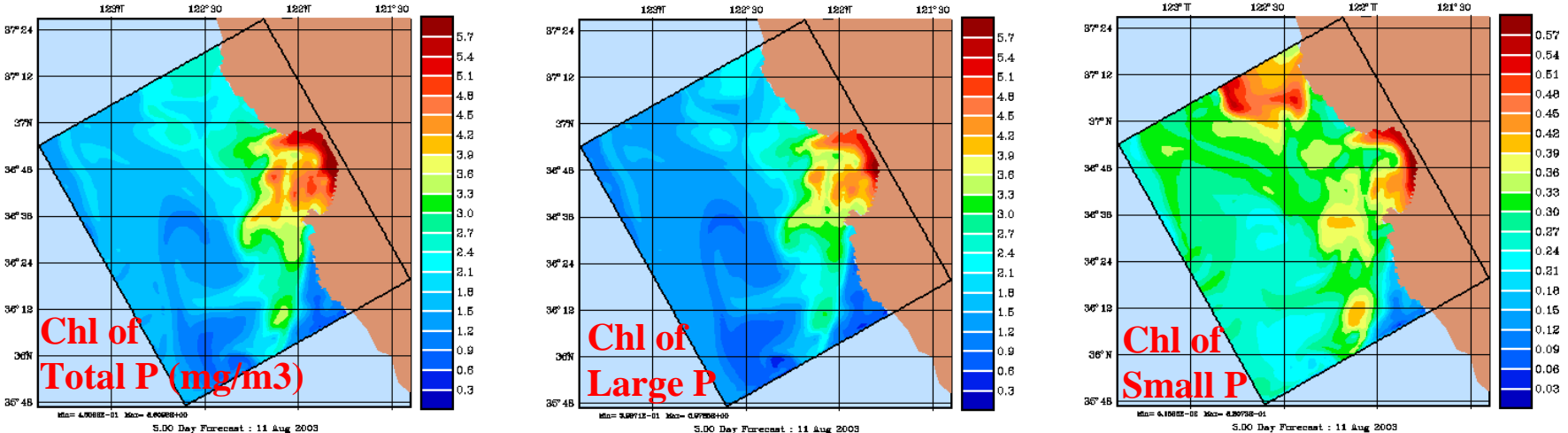
Function	References
(1) Rectilinear $g_i = \begin{cases} g_{\max} \frac{p_i P_i}{K}, & \text{for } R \leq K \\ g_{\max}, & \text{for } R > K \end{cases}, \quad R = \sum_{i=1}^n p_i P_i$	Armstrong, 1994
(2) Ivlev function for each prey type: $g_i = g_{\max} (1 - e^{-a_i P_i})$	Leonard et al., 1999
(3) Ivlev function with interference between prey types: $g_i = g_{\max} (1 - e^{-a_i R}) \frac{p_i P_i}{R}, \quad \text{with } R = \sum_{i=1}^n p_i P_i$	Hofmann and Ambler, 1988
(4) Mechanistic disc function: $g_i = g_{\max} \frac{a_i N_i}{1 + \sum_{j=1}^n a_j \tau_j N_j}$	Murdoch and Oaten, 1975; Holt, 1983; Gismervik and Anderson, 1997; Strom and Loukos, 1998
(5) Michaelis Menten Function: $g_i = g_{\max} \frac{p_i P_i}{K + \sum_{j=1}^n p_j P_j}$	Murdoch, 1973; Real, 1977; Moloney and Field, 1991; Verity, 1991; Gismervik and Anderson, 1997; Strom and Loukos, 1998
(6) Threshold MM function: $g_i = g_{\max} \left(\frac{R - P_0}{K + R - P_0} \right) \frac{p_i P_i}{R}, \quad \text{with } R = \sum_{j=1}^n p_j P_j$	Evans, 1988; Lancelot et al., 2000
(7) Modified MM function: $g_i = g_{\max} \frac{p_i P_i}{1 + \sum_{j=1}^n p_j P_j}$	Verity, 1991; Fasham et al. (1999) and Tian et al. (2001)

Table 2. Parameterization of grazing on multiple types of prey with active switching selection (g_{max} : maximum grazing rate; K: Half-saturation constant; P_0 threshold below which grazing is zero; p_i : preference coefficient; α , a , τ : constant).

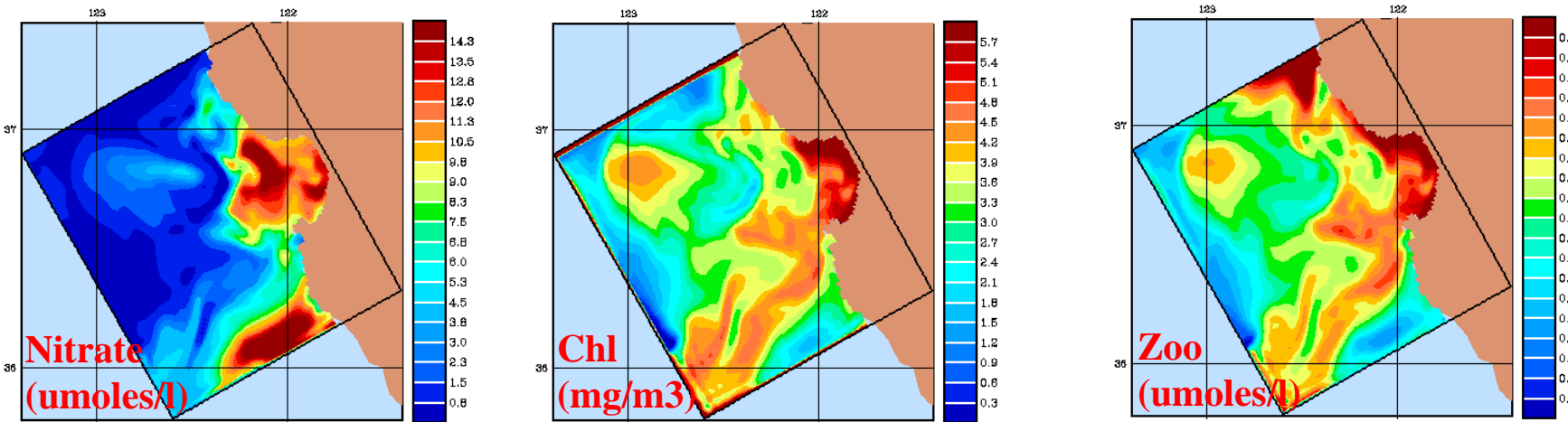
Function	References
(1) Switching MM predation: $g_i = g_{\max} \frac{p_i P_i^2}{K \sum_{j=1}^n p_j P_j + \sum_{j=1}^n p_j P_j^2}$	Fasham et al., 1990; Strom and Loukos, 1998; Pitchford and Brindley, 1999; Spitz et al., 2001
(2) Mechanistic disc switching predation: $g_i = g_{\max} \frac{b_i N_i^2}{(1 + c_i N_i)(1 + \sum_{j=1}^n \frac{b_j h_j N_j^2}{1 + c_j N_j})}$	Chesson, 1983
(3) Generalized switching function: $g_i = g_{\max} a_i \frac{(p_i P_i)^m}{\sum_{i=1}^n (p_i P_i)^m}$	Tansky, 1978; Teramoto, 1979; Matsuda et al., 1986
(4) Generalized switching function: $g_i = g_{\max} \frac{(p_i P_i)^m}{\left(\sum_{i=1}^n (p_i P_i) \right)^m}$	Vance, 1978
(5) Generalized switching MM function: $g_i = g_{\max} \frac{(p_i P_i)^m}{1 + \sum_{i=1}^n (p_i P_i)^m}$	Gismervik and Andersen (1997)
(6) Generalized switching MM function: $g_i = g_{\max} \frac{(p_i (P_i - P_{0i}))^m}{1 + \sum_{i=1}^n (p_i (P_i - P_{0i}))^m}$	This work

Towards automated quantitative model aggregation and simplification

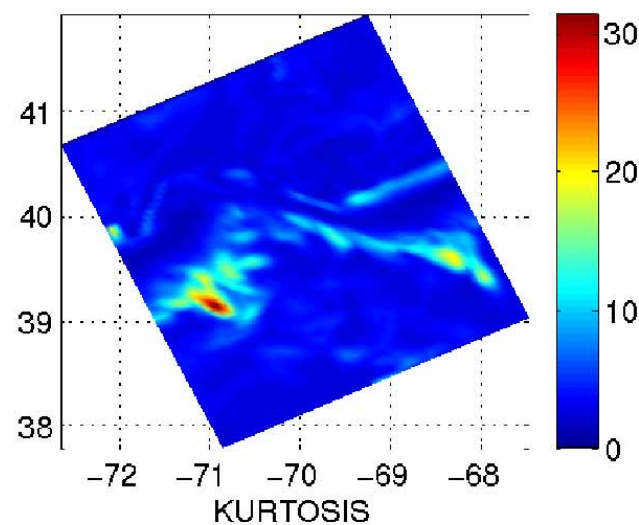
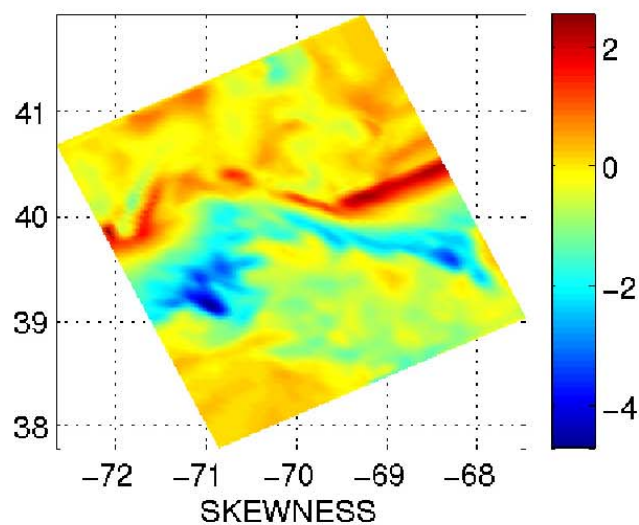
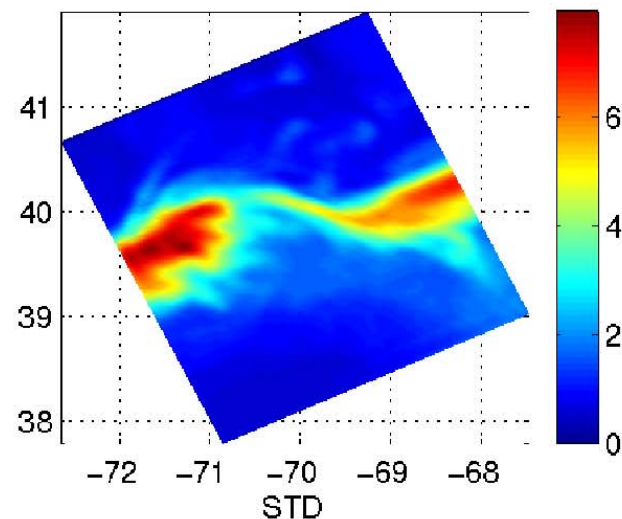
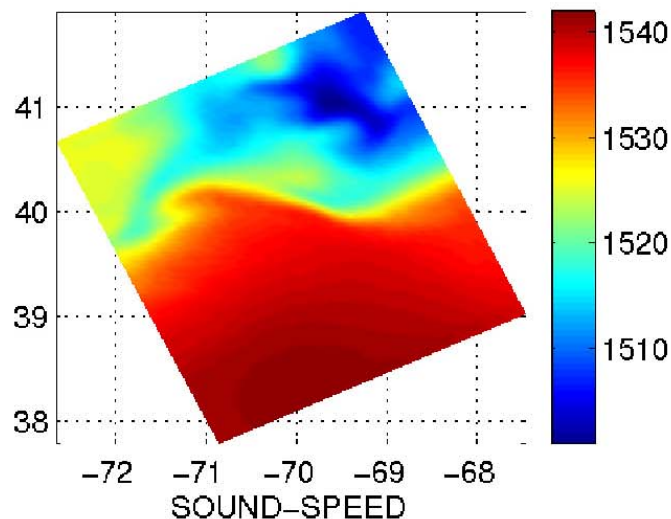
A priori configuration of generalized model on Aug 11 during an upwelling event



NPZ configuration of generalized model on Aug 11 during same upwelling event



Environmental-Acoustical Uncertainty Estimation and Transfers, Coupled Acoustical-Physical DA and End-to-End Systems in a Shelfbreak Environment



COUPLED PHYSICAL-ACOUSTICAL DYNAMICAL MODELS

• Physical model: Primitive-Equation (PDE, x, y, z, t : HOPS)

$$\text{Horiz. Mom.} \quad \frac{D\mathbf{u}_h}{Dt} + f \mathbf{e}_3 \wedge \mathbf{u}_h = -\frac{1}{\rho_0} \nabla_h p_w + \nabla_h \cdot (A_h \nabla_h \mathbf{u}_h) + \frac{\partial A_v}{\partial z} \frac{\partial \mathbf{u}_h}{\partial z} \quad (1-2)$$

$$\text{Vert. Mom.} \quad \rho g + \frac{\partial p_w}{\partial z} = 0 \quad (3)$$

$$\text{Thermal en.} \quad \frac{DT}{Dt} = \nabla_h \cdot (K_h \nabla_h T) + \frac{\partial K_v}{\partial z} \frac{\partial T}{\partial z} \quad (4)$$

$$\text{Cons. of salt} \quad \frac{DS}{Dt} = \nabla_h \cdot (K_h \nabla_h S) + \frac{\partial K_v}{\partial z} \frac{\partial S}{\partial z} \quad (5)$$

$$\text{Cons. of mass} \quad \nabla \cdot \mathbf{u} = 0 \quad (6)$$

$$\text{Eqn. of state} \quad \rho(\mathbf{r}, z, t) = \rho(T, S, p_w) \quad (7)$$

$$\text{Sound speed eqn.} \quad c(\mathbf{r}, z, t) = C(T, S, p_w) \quad (8)$$

• Acoustical model: Coupled Normal-Mode model (PDE, f, r, z, t : NPS)

$$\text{Wave eqn.} \quad \rho c^2(\mathbf{r}, z, t) \nabla \cdot \left(\frac{1}{\rho} \nabla p_s(\mathbf{r}, z, t) \right) = \frac{\partial^2 p_s(\mathbf{r}, z, t)}{\partial t^2}$$

$$\text{Pres. transfer fct.} \quad \nabla^2 P_s - \frac{1}{\rho} \nabla \rho \cdot \nabla P_s + k^2 P_s = -2 \frac{r_0}{r} \delta(r-r_0)(z-z_0)$$

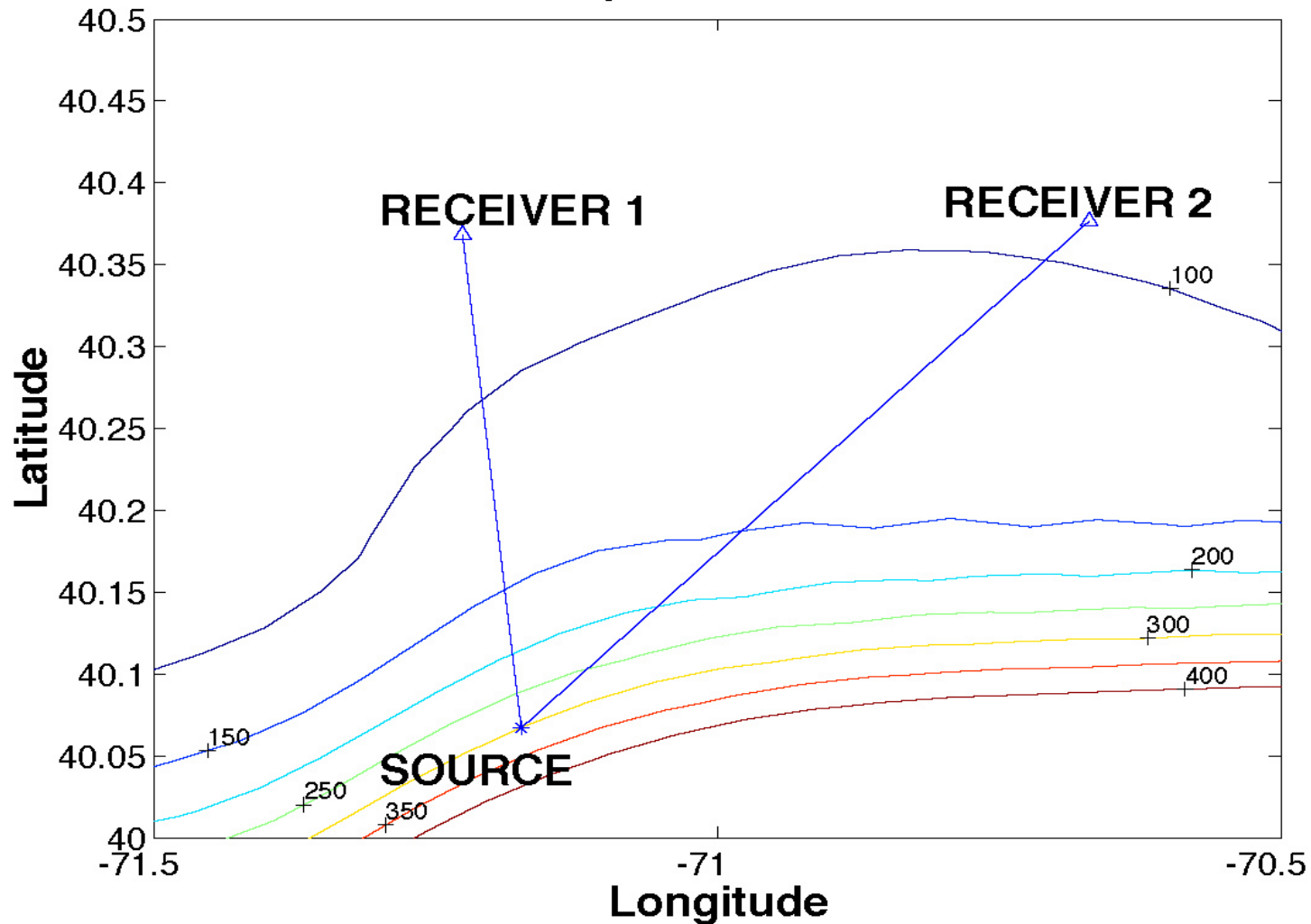
$$\text{where } k \doteq 2\pi f / c(\mathbf{r}, z, t) \quad (9)$$

$$\text{Coupled} \quad \text{With } P_s(r, z; f) \doteq \sum_n \frac{r_0}{\sqrt{r}} P_n(r; f) Z_n(z; r, f) \quad (10)$$

$$\text{Normal-modes} \quad \left\{ \frac{\partial^2}{\partial z^2} - \frac{1}{\rho(r, z)} \frac{\partial \rho(r, z)}{\partial z} \frac{\partial}{\partial z} + (k(r, z)^2 - k_n(r; f)^2) \right\} \\ \times Z_n(z; r, f) = 0 \quad (11)$$

$$\text{Modal amplit.} \quad \left(\frac{d^2}{dr^2} + k_n^2 \right) P_n = - \sum_m (\gamma_{mn} \frac{d}{dr} + C_{mn}) P_m \quad (12)$$

Simulation Experiment Acoustic Paths

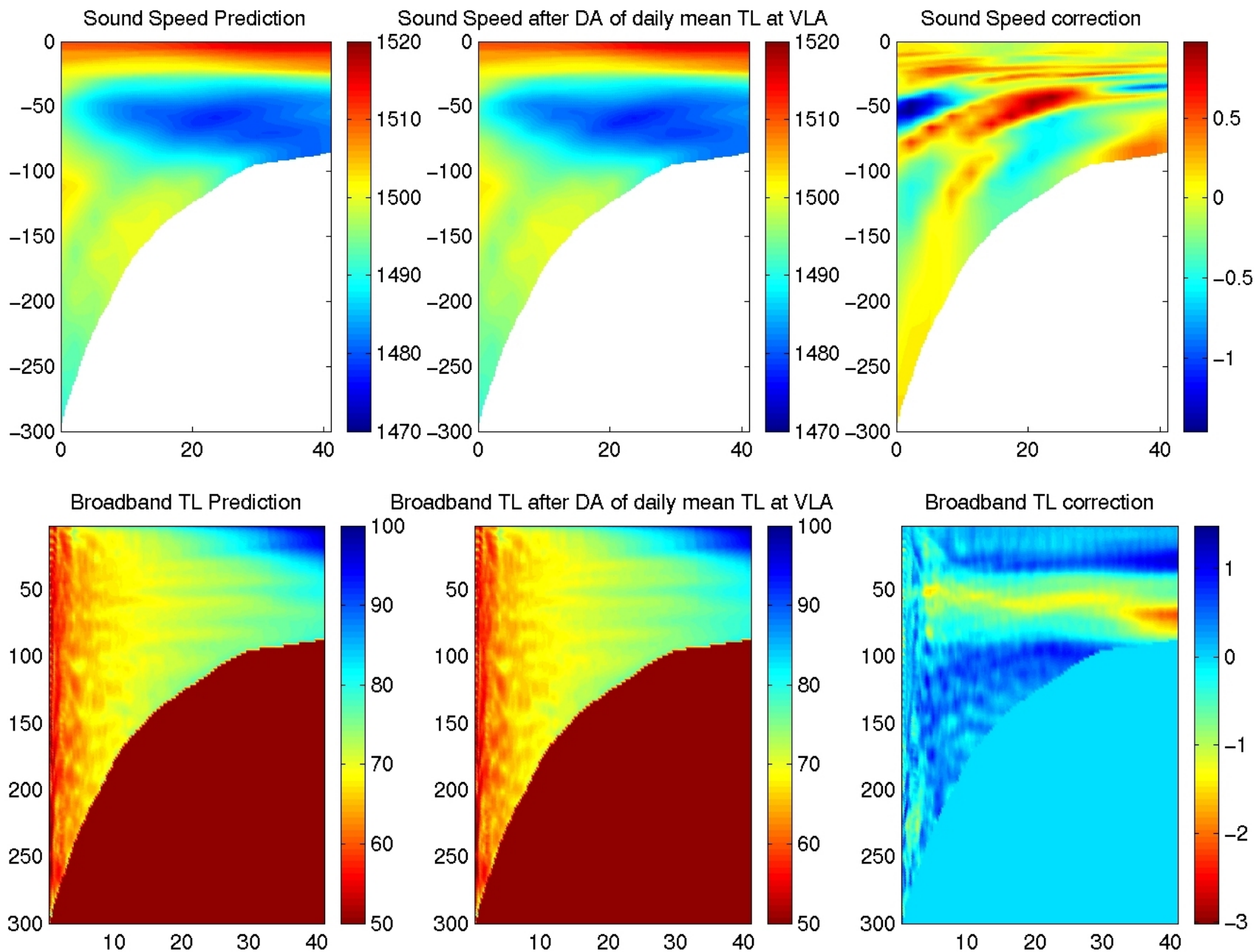


Shelfbreak-PRIMER Acoustic paths considered, overlaid on bathymetry.

Path 1:

- **Source:** at 300m, 400 Hz
- **Receiver:** VLA at about 40 km range, from 0-80m depths

Coupled Physical-Acoustical Data Assimilation of real TL data



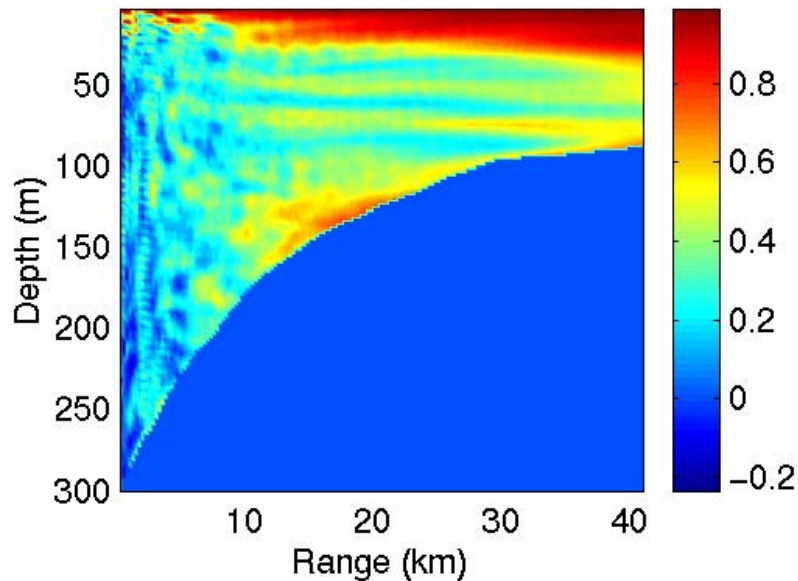
Data Acquisition for Parameter estimation:

Bottom inference via optimal adaptive ocean-acoustic sampling

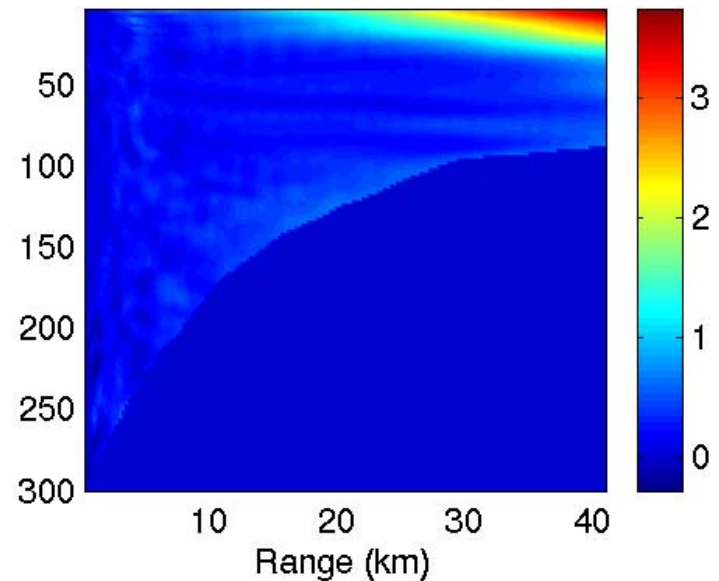
The correlation/covariance fields below are computed using ESSE and CS's code.

For a 400Hz source at 300m depth, they show where one should measure TL and take an ocean profile to best estimate the bottom attenuation coefficient

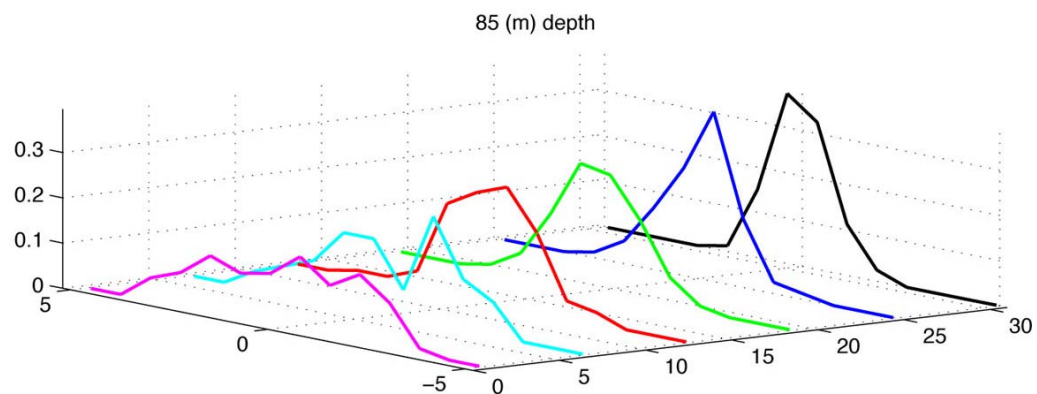
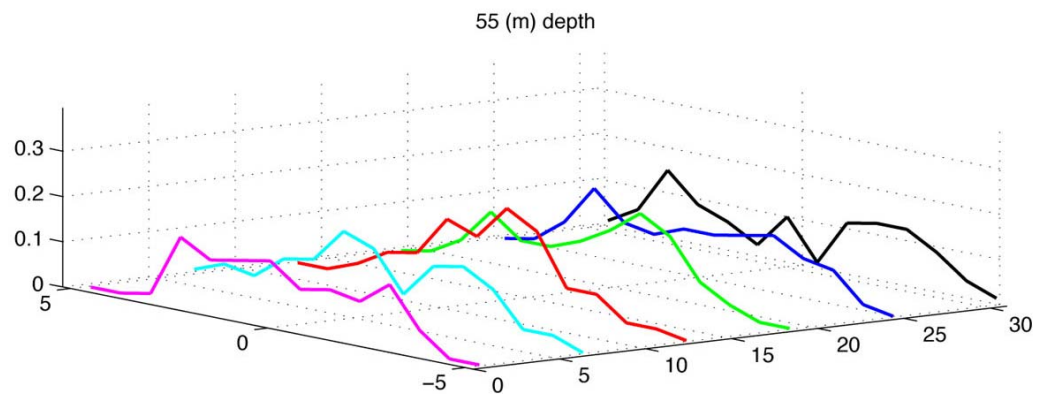
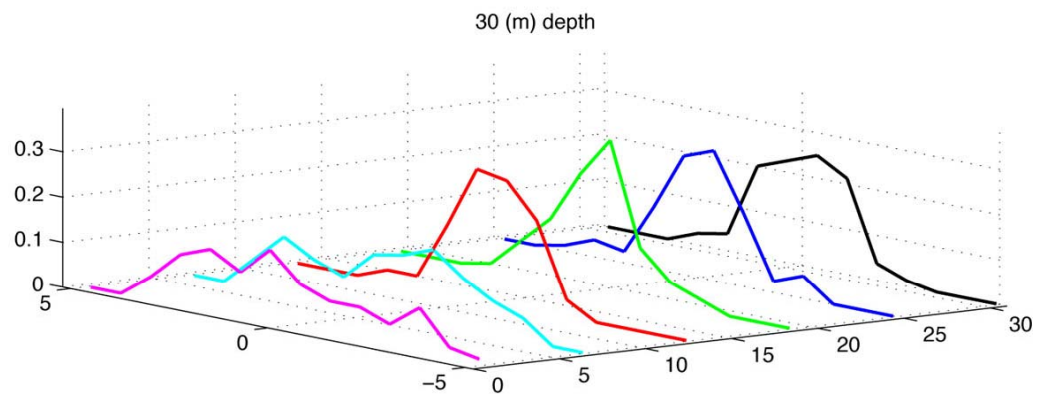
Correlation between TL and bot. att. coef.



Covariance between TL and bot. att. coef.



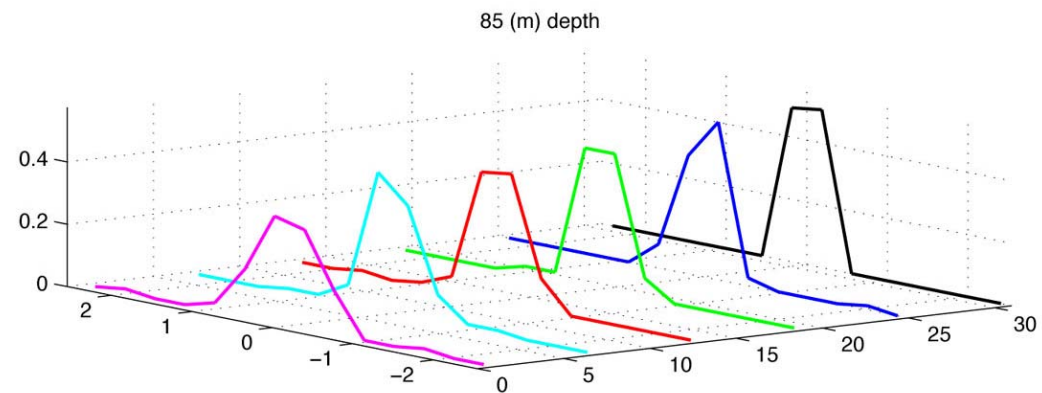
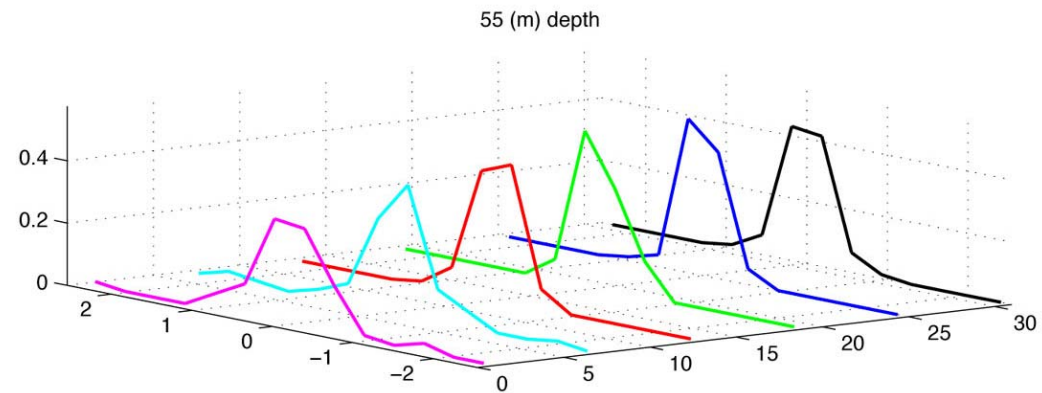
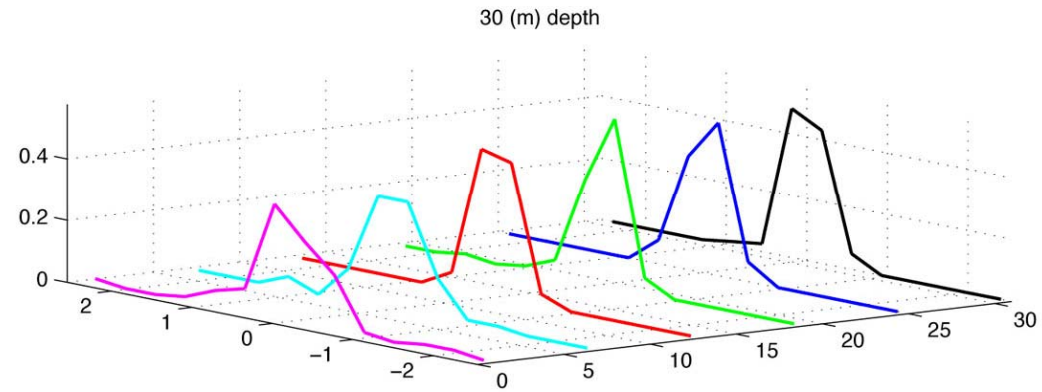
Predicted PDF of broadband TL



TL dev. from mean (db)

Range (km) - Log scale

After Assimilation PDF of broadband TL



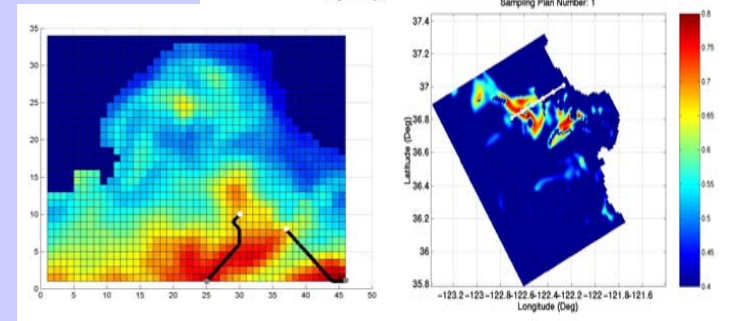
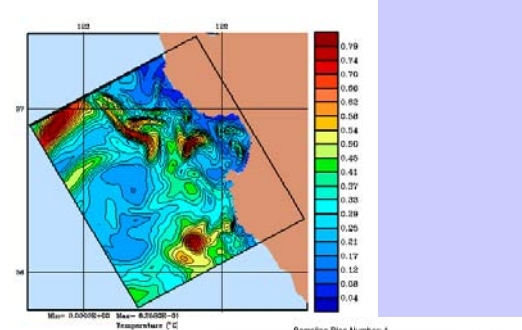
TL dev. from mean (db)

Range (km) - Log scale

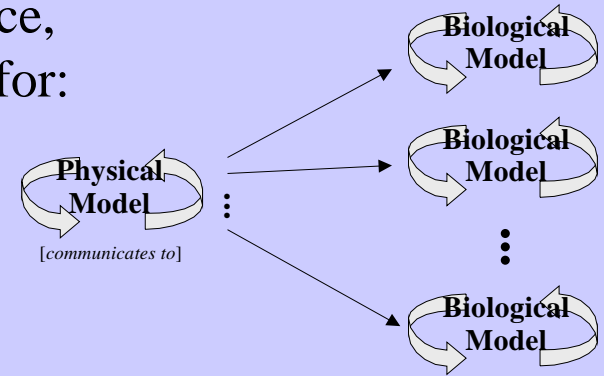
CONCLUSIONS

- ESSE useful nonlinear scheme for interdisciplinary estimation of oceanic state variables and error fields via multivariate physical-biogeochemical-ecosystem-acoustical data assimilation

- AOSN-II: Real-time Consistent Error Forecasting, Data Assimilation and Quantitative Adaptive Sampling in Monterey Bay for 1 month (first time)



- New era of fully interdisciplinary oceanic system science, combining models and data, with (math) opportunities for:
 - Adaptive modeling/system identification (parameters, structures, state-variables, errors)
 - Adaptive sampling
 - Adaptive model reductions and simplifications
 - Dynamical balances and quantitative process studies



- PRIMER: Environmental-acoustical uncertainty estimated and transferred, and Acoustical-physical DA carried-out. Leads End-to-end (physical-geological-acoustical-sonar-noise) system for advanced sonar performance prediction

